Forearc Crustal Structure of Ecuador Revealed by Gravity and Aeromagnetic Anomalies and Their Geodynamic Implications

Carlos Aizprua, C. Witt, M. Brönner, S. E Johansen, D. Barba, M. J Hernandez

GeoScienceWorld
Lithosphere
Volume 2020, Article ID 2810692, 23 pages
https://doi.org/10.2113/2020/2810692

Lithosphere

Research Article

Forearc Crustal Structure of Ecuador Revealed by Gravity and Aeromagnetic Anomalies and Their Geodynamic Implications

Carlos Aizprua,[1,2,3] **C. Witt**,[2] **M. Brönner**,[1,4] **S. E. Johansen**,[1] **D. Barba**,[5] **and M. J. Hernandez**[6,7]

[1]*Department of Geoscience and Petroleum, Norwegian University of Science and Technology (NTNU), S.P. Andersens Veg 15a, 7491 Trondheim, Norway*
[2]*Univ. Lille, CNRS, Univ. Littoral Côte d'Opale, UMR 8187, LOG (Laboratoire d'Océanologie et de Géosciences), F 59000 Lille, France*
[3]*Facultad de Ingeniería en Ciencias de la Tierra, Escuela Superior Politécnica del Litoral, Campus Gustavo Galindo, Km 30.5 Vía Perimetral, Guayaquil, Ecuador*
[4]*Geological Survey of Norway (NGU), Leiv Eirikssons Vei 39, 7040 Trondheim, Norway*
[5]*Petroamazonas EP, Av. 6 de Diciembre N34-290 y Gaspar Cañero, Edificio Villafuerte, Quito, Ecuador*
[6]*Université Côte d'Azur, IRD (Institut de Recherche Pour Le Développement), Sorbonne Université, Centre National de la Recherche Scientifique (CNRS), Observatoire de la Côte d'Azur, GEOAZUR (Laboratoire de Géoazur), 06560 Valbonne, France*
[7]*Departamento de Geología, Escuela Politécnica Nacional, Quito, Ecuador*

Correspondence should be addressed to Carlos Aizprua; calun@equinor.com

Received 28 January 2020; Accepted 5 October 2020; Published 16 November 2020

Academic Editor: Andrea Billi

Along the Western Cordillera of Ecuador, fault-bounded ophiolites derived from the Late Cretaceous Caribbean Large Igneous Province (CLIP) have provided key petrotectonic indicators that outline the nature and the mechanism of continental growth in this region. However, most of the forearc basement across Western Ecuador is buried under sediments impairing its crustal structure understanding. Here, we propose a first crustal model throughout the spectral analysis of gravity and aeromagnetic data, constrained by observations made both at the surface and at the subsurface. Three main geophysical domains, within the North Andean Sliver in Western Ecuador, have been defined based on spectral analysis and augmented by 2D forward models. An outer domain, characterized by magnetic anomalies associated with mafic rocks, coincides with evidence of a split intraoceanic arc system. An inner domain is governed by long-wavelength mid to deep crust-sourced gravity and magnetic anomalies possibly evidencing the root of a paleoisland arc and the residuum of a partial melting event with subsequent associated serpentinization, the latest possibly associated with an obduction process during the middle Eocene-Oligocene. In addition, our model supports the presence of a lithospheric vertical tear fault, herein the southern suture domain, inherited from an oblique arc-continent interaction. Our interpretation also brings new insights and constraints on the early geodynamic evolution of the Ecuadorian forearc and provides evidence on the structural style and preservation potential of the forearc basement, most likely the roots of a mature island arc built within an oceanic plateau.

1. Introduction

Major continental growth took place along the NW corner of South America during the Late Cretaceous, following the collision and accretion of a sliver from the Caribbean Large Igneous Province (CLIP) [1–3]. Records of the interaction between the CLIP and the South America continental margin are preserved along its suture zone in the Western Cordillera and in SW coastal Ecuador (e.g., [4–8]) (Figure 1). Several lines of evidence suggest that prior to the collision with South America, the CLIP was affected by the emplacement of the tholeiitic San Lorenzo/Naranjal and Rio Cala island arcs, while the western limit of the South American Plate (SAP) was most likely a passive margin [6, 8]. Different authors agree on an oblique arc-passive margin collision configuration starting at ~75 Ma [1, 6, 9] with subsequent clockwise

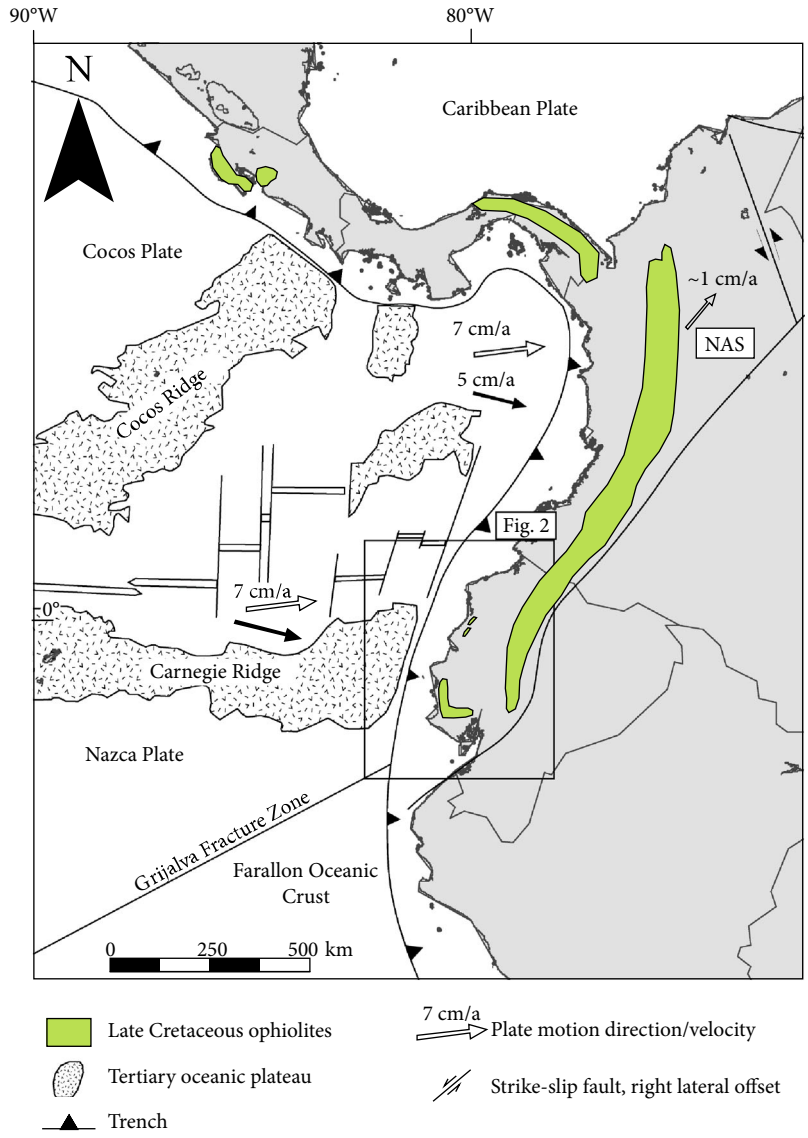

FIGURE 1: Plate configuration of the NW South America and Central America regions, highlighting the surface exposure of ophiolites attributed to the Late Cretaceous Caribbean Large Igneous Province (CLIP). Plate kinematics are derived from relative plate motions according to GPS data (unfilled color arrow) and the NUVEL-1 global kinematic model (filled color arrow). Modified after [3, 52, 107].

block rotations between ~70 and 75 Ma [2, 10, 11]. However, discrepancies exist about the subduction polarity beneath the CLIP. This aspect and the arc-continent collision geometry, including the tectonic regime of the subduction, may have had a great impact on the preferential preservation or loss of evidence of the Late Cretaceous subduction system [12].

Stern et al. [13] suggest that ophiolites emplaced along the suture zone provide the best record for understanding subduction initiation processes and forearc composition and magmatic stratigraphy. Such exposures along the Western Cordillera of Ecuador and Colombia have provided key petrotectonic indicators for the geodynamic reconstruction of the NW South American margin (Figure 1). Nevertheless, the low preservation potential of such ancient terranes after an arc-continent collision, together with limited exposure, could limit geodynamic reconstructions, leading to controversial interpretations [12, 14]. Despite the records of arc activity in the Western Cordillera, there are few publications discussing the different precollision elements of the subduction system including the location of the trench, forearc, and back-arc systems.

In Western Ecuador, between the Coastal Cordillera and the Western Cordillera (Figure 2(a)), the units associated with the accreted sliver are buried beneath the Cenozoic forearc sediments impairing the reconstruction of the underlying forearc basement. We use an unpublished aeromagnetic/-gravity survey of this region (Figure 2(b)) and present a multiscale data integration approach to uncover the underlying crustal structure of the forearc region in Ecuador and add further constraints on the geodynamic evolution of the region. This work was motivated by the lack of a crustal model for the Ecuadorian forearc region. Indeed, since the presentation of a simple 2D Bouguer's anomaly forward model across the continental margin by Feininger and Seguin

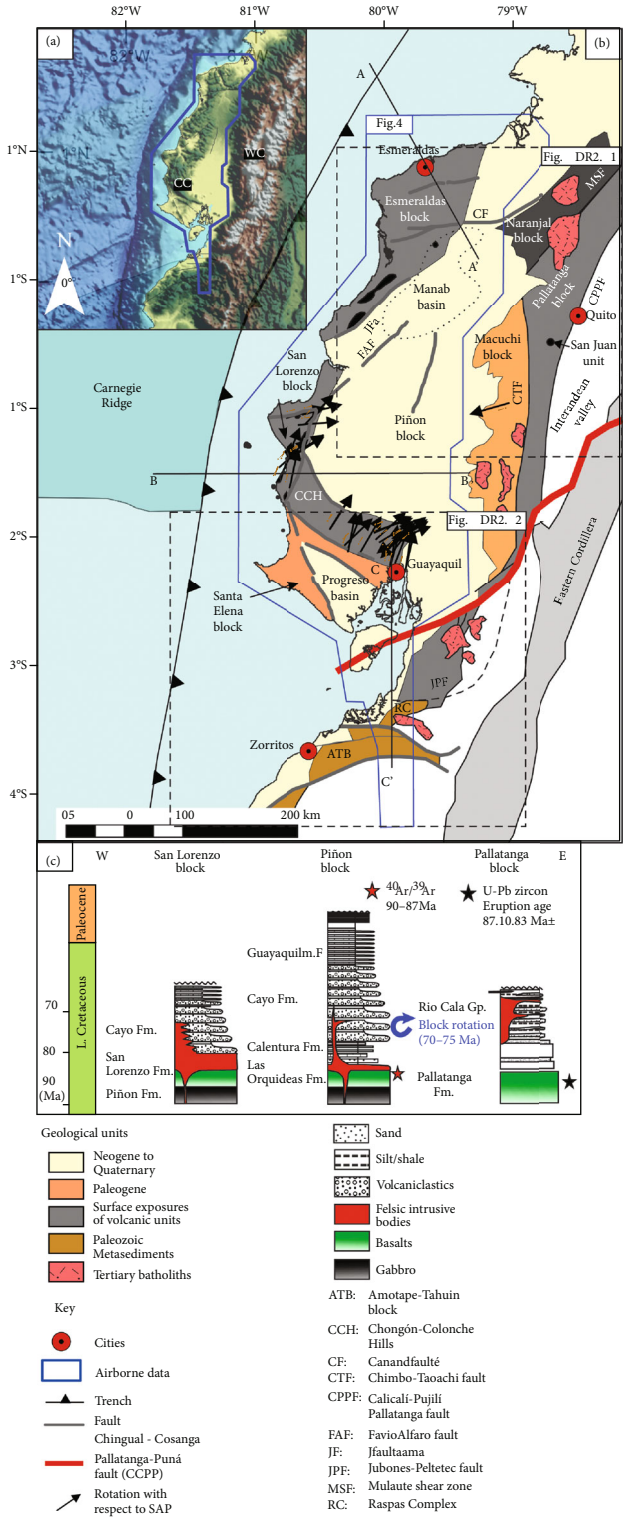

FIGURE 2: (a) Topographic relief map of western Ecuador and NW Peru showing the location and coverage of the aeromagnetic survey. (b) Simplified tectonic terrane map showing the different crustal blocks interpreted along western Ecuador maps (modified after Luzieux et al. [10] and Vallejo et al. [8]). The blue outline defines the limits of the gravity and magnetic aeromagnetic survey used in this study. (c) Representative stratigraphic columns for the three main tectonic blocks discussed in this study.

[15], and a more recent and similar plate-scale study using satellite potential field data by Tamay et al. [16], the underlying basement structure of the Ecuadorian forearc remains poorly understood.

In this work, we have defined three main geophysical domains based on the analysis of aerogravity/magnetic anomalies, constraints derived from published geodynamic scenarios [6–8, 10, 17, 18], and by means of 2D forward models. Our interpretation shows a heterogeneous and structurally complex basement, which may have resulted from the fragmentation of the sliver following the initial Late Cretaceous accretionary phase. Furthermore, our model sheds light on the nature of the southern suture between the accreted sliver of the CLIP and the continental block.

2. Regional Geology

The Coastal and Western Cordillera regions in Ecuador are characterized by exposures associated with crustal fragments derived from the plume-derived Caribbean Large Igneous Province (CLIP) erupted in Early-Late Cretaceous times (e.g., [3, 18, 19]) (Figure 2). The arrival and collision of the CLIP along the NW corner of the South American margin have been dated as a Late Cretaceous event (75-65 Ma) on the basis of stratigraphic, paleomagnetic, and radiometric age control [7, 8, 20]. Paleomagnetic studies in Western Ecuador by Roperch et al. [11] and Luzieux et al. [10] concluded that the arc-derived basement in Ecuador was generated at low latitudes. The collision of the CLIP may have been followed by crustal fragmentation and clockwise rotations (ca. 40-50°) during the Campanian to Early Maastrichtian [10, 11]. Alternative models propose the presence of at least two different oceanic plateaus emplaced during two accretionary periods between the Late Cretaceous and the Late Eocene [5, 7, 21, 22].

2.1. Western Cordillera Crustal Blocks

2.1.1. Pallatanga Block. The block is located along the Western Cordillera, composed of a series of fault-bounded slices with SSW-NNE direction (Figure 2(b)). It is limited to the west by the Chimbo-Toachistrike slip fault and to the east by the Calacalí-Pujilí-Pallatanga fault, which represents part of the Late Cretaceous ocean-continent suture [8] (Figure 2(b)). It comprises Early to Late Cretaceous mafic to ultramafic rocks, mainly composed of basalts, gabbros, and massive dolerites, overlain by volcanic lastic sediments (Figure 2(c)) [7, 18]. Basalts and gabbros from the Pallatanga block have an enriched MORB geochemical signature, possibly related to a mantle plume [5, 7, 18, 23, 24]. Its easternmost part comprises serpentinized peridotites, dolerites, and hornblende-bearing gabbros from the San Juan unit [6, 7]. An amphibole-bearing gabbro of this unit yielded an Sm/Nd isochron of 123 ± 1.3 Ma [23] and a poor Ar/Ar integrated age of 105 Ma [25]. However, zircons from a layered gabbro mapped as the San Juan unit yielded a U/Pb age of 87.1 ± 1.66 Ma [8], suggesting that the San Juan unit is part of the same oceanic plateau as the Pallatanga unit.

2.1.2. Macuchi Block. The Macuchi block is in faulted contact with the Pallatanga block along the Chimbo-Toachi fault (Figure 2(b)) [7, 8]. Different authors have interpreted the Macuchi block as a volcanic arc accreted during the Eocene (e.g., [7, 17]). However, Vallejo et al. [8] suggest that this is a difficult model to reconcile given the current position of the Macuchi block, in between the Pallatanga and Piñón blocks that possess a similar radiometric age (ca. 88 Ma).

The Macuchi block is mostly characterized by volcaniclastic material with a small percentage of basaltic pillow lavas, lithic tuffs of basaltic and andesitic composition, basaltic breccias, turbidites of volcanic origin, and cherts [5, 26]. The sedimentary units that compose the Macuchi block are interpreted as a product of submarine volcanism transported by gravity flow processes [5]. Whole-rock K/Ar radiometric data yield an age of 41.6 ± 2.1 Ma for a basaltic andesite sample [27]. Vallejo et al. [8] obtained a similar age of 42.63 ± 1.3 Ma from a plagioclase of an andesitic lava flow. Nevertheless, the age of the base of the Macuchiunit, as well as the age of the volcaniclastic deposits, remains largely unconstrained.

2.1.3. Naranjal Block. The block is located in the northern part of the study area in faulted contact with the Pallatanga block, along the Mulaute shear zone (Figure 2(b)). The Naranjal block is characterized by rocks with a volcanic arc affinity, which appears to correlate with the interpreted Ricaurte arc in southern Colombia [28]. It is composed of basaltic pillow lavas and andesites with intercalated sedimentary rocks [26]. Two distinct lithotectonic units have been interpreted within the block: (1) island arc lavas, towards the north, which may correlate with basalts from the Río Cala group at the Pallatanga block, and (2) to the south by rocks with plateau affinities [7]. The southern extent of the Naranjal block is assumed to be buried under the forearc sediments of the Manabí basin (Figure 2(b)).

2.2. Volcanic and Oceanic Plateau Remnants in the Forearc Region

2.2.1. Piñón and Santa Elena Blocks. The exposures in the Chongón Colonche Hills in SW Ecuador (Figure 2(a)) are mainly composed of tholeiitic basalts, pillow lavas, and gabbros. The geochemical signature of these mafic rocks supports an oceanic plateau interpretation [7, 18, 21, 22].

The age of the Piñón Formation was initially constrained by foraminifera and nannofossils from the overlying black shales of the Calentura Formation, which yielded a Cenomanian-Early Coniacian age and led Reynaud et al. [22] to propose an Early Cretaceous age for the Piñón Formation. Van Melle et al. [19] then based on an expanded stratigraphic dataset propose a Coniacian age for the Piñón Formation. Furthermore, it was suggested that the Pallatanga and Piñón blocks were fragmented after the Late Cretaceous collision with the South American margin. This is supported by $^{40}Ar/^{39}Ar$ dating yielding an age between 90 and 87 Ma for both crustal blocks [10].

South of the Chongón-Colonche Hills, in the Santa Elena block (Figure 2), the stratigraphy is dominated by deformed Late Cretaceous rocks from the Santa Elena Formation, unconformably overlain by folded rocks from the Paleocene Azúcar Formation. These deformed sequences are interpreted as an accretionary wedge, which led to the development of an outer forearc high during the Oligocene, and the development of the restricted Neogene Progreso basin (Figure 2(b)) [4, 29]. It is assumed that volcaniclastic sequences from the Cayo Formation and possibly mafic rocks from the Piñón Formation form the underlying basement of the Santa Elena block.

2.2.2. San Lorenzo Block. Located to the west of the Piñón block and delimited by the Jipijapa, Jama, and Canandé faults (Figure 2(b)), this block forms the medium topography (max. 400 m) Coastal Cordillera [30]. The mafic rocks exposed in the Coastal Cordillera are attributed to the Piñón Formation, commonly overlain by coarse-grained sandstones, ash beds, basaltic flows, dikes, and pillow lavas (Figure 2(c)) [10, 22]. Goossens and Rose [31] report that tholeiites erupted along east-trending fractures from the Late Cretaceous until Early Eocene. These rocks are attributed to a Campanian to Maastrichtian volcanic island arc constituting the San Lorenzo Formation [8, 19, 21, 22]. Based on plagioclase from pillow basalts Ar/Ar dated as 72.7 ± 1.4 Ma, Lebrat et al. [17] proposed that the island arc-related sequences preserved in the Coastal and the Western Cordillera are coeval and possibly part of the same system. However, several authors report larger age ranges between 87 and 54 Ma [10, 21, 31]. The San Lorenzo block is also characterized by a clear hiatus between the Late Cretaceous and Middle Eocene carbonaceous formations [10, 22, 32], which has been attributed to the accretion of the San Lorenzo block to the already accreted Piñon block, during Paleocene-Eocene times [7, 21].

2.2.3. Esmeraldas Block. Limited to the east by the Canandé fault and mostly covered by Neogene sediments (Figure 2(b)), this is the least well-constrained block in terms of its nature and age. It is composed of pillow basalts, dolerites, isotropic gabbross, and hyaloclastites containing glass fragments and picritic compositions [18]. The same authors suggest that the units forming the block appear petrologically and geochemically like the lavas of the CLIP (92-86 Ma).

2.3. Amotape-Tahuin Massif along NW Peru. The Amotape-Tahuin Massif is an E-W oriented morphological feature composed of Precambrian to Paleozoic rocks along the NW coast of Peru, which shifts into a N-S direction towards the south [33]. Towards the ENE, the Jubones fault separates rocks with a continental affinity from those composed of exhumed high pressure, low-temperature oceanic origin [34–36].

Most of the massif between 4°S to 6°S is composed of metasediments. Zircon ages along the metamorphic belt show a very similar pattern of Neoproterozoic age clusters and a younger group around 320 Ma and suggest a common metasedimentary origin of the entire massif [37]. Furthermore, these age clusters are similar with those in the western parts of the Eastern Cordillera and the northern section of the Occidental Cordillera of Peru suggesting a wide,

polyphase Andean metamorphic belt [37] thus excluding previous theories about the allochthonous origin for the Amotape-Tahuin Massif [33, 38, 39]. Moreover, its autochthonous origin was previously evidenced by the pervasive presence of Triassic (230-220 Ma) granitoids along the Amotape Massif and the Cordillera Real of Ecuador [35, 40, 41].

Paleomagnetic studies at the Amotape-Tahuin Massif report clockwise rotations in the order of 35° during the Late Cretaceous-Early Paleocene, related to the collision and accretion of the CLIP [33]. Fault mapping and displacement data show deformation that might be associated with a post-Paleocene reactivation, with block rotations in the order of 25° [42], of the inherited structures formed during the initial accretionary phase [4].

3. Previous Gravimetric and Magnetometric Studies

The earliest study using aeromagnetic data was carried out during the mid-1960's for the Mineral Project of the United Nations Development Program [31] and identified a series of E-W magnetic anomalies, along the San Lorenzo block, bounded to the west by a major north to NE-trending fault (Jipijapa fault in this study). Goossens and Rose [31] suggest that these anomalies are caused by tholeiitic basaltic flows (their "Basic Igneous Complex"). Later, these rocks were compared to similar exposures in Colombia and interpreted to form an elongated igneous belt along the NW of South America, from Ecuador to Panamá [43]. Subsequent potential field studies along the margins of Ecuador and Peru analyzed free-air gravity gradients, both near the trench and along the continental slope [44]. Primary observations along the NW Peru and SW Ecuador margin by Shepherd and Moberly [44] include (1) flattened gradients east of the current trench position associated with a wedge of tectonized sediments accumulated by subduction processes; (2) abrupt free-air gravity inflections on the upper slope (NW Peru), related to granitic basement (correlative to the Amotape-Tahuin block); and (3) a gravity minimum in the Gulf of Guayaquil, which denotes more than 6000 m of Quaternary sediments infilling an inferred pull-apart basin.

Feininger and Seguin [15] characterized the crust in Ecuador using a 2D forward model (located at ~2°S) based on simple Bouguer gravity data. They concluded that the coastal region in Ecuador must be underlain by an ancient oceanic plate. Based on the correlation between positive (Bouguer) anomalies over the inferred oceanic terrane and negative values over the interpreted continental crust, they proposed a possible location for the suture between these two crustal blocks. Nevertheless, the conclusions drawn for the coastal region lacked a more thorough analysis regarding its internal structure.

Tamay et al. [16] studied the extension of the subducted Carnegie Ridge using potential field data analysis and suggest that the Carnegie Ridge underlies the continental margin reaching the Andes Cordillera based on an elongated E-W negative magnetic anomaly concordant with the position of the aseismic ridge and that it subsequently controlled margin segmentation, seismicity, and volcanism. Free-air gravity anomalies along the offshore zone have more recently been used to constrain the tectonic development of the offshore forearc basins between 1°N and 2°S [45]. This study shows a clear relationship between depth-to-basement and related faulting and the distribution of gravimetric anomalies.

Despite the different studies using potential field data, none of them present a detailed view of the crustal structure of the entire forearc region in Ecuador. Utilizing recently acquired high-resolution aeromagnetic and gravity data along the coastal region, we present a model of the underlying crustal architecture of the forearc region in Western Ecuador.

4. Geophysical Data and Methods

An aeromagnetic/gravity survey, acquired by Sander Geophysics for EP Petroecuador in 2010, is available between 2°N and 4°S for the forearc region in Ecuador (Figure 2). A total area of ca. 78000 km^2 was covered with N-S oriented acquisition lines and E-W tie lines with a spacing of ca. 1500 m and ca. 8950 m, respectively, and a nominal flight altitude of 250 m above the terrain. In addition, we had access to unpublished onshore seismic lines acquired and processed by Sinopec for EP Petroecuador in 2009, which aid to define the forearc basin geometry (especially depth to basement) within the study area. Offshore seismic reflection and refraction profiles across the margin [45–49] were integrated into the 2D models to constrain the extent of the forearc basement up to the trench.

4.1. Analysis of Gravity and Magnetic Anomalies. Our approach is based on two steps: (1) a spectral analysis of the frequency content to map out buried geological features and (2) 2D forward modeling of the anomalies to test plausible geological scenarios. Throughout this approach, we aim to delineate the main geophysical domains and to characterize the interpreted crustal blocks in terms of density and magnetic susceptibility.

Conventional filtering techniques including regional and residual anomalies, analytical signal, and tilt derivative were applied to the data (Item DR1), in order to aid geological interpretations of the sources of the gravity and magnetic anomalies. Due to the poor coverage and low-frequency content of global satellite-derived magnetic data in this region, only the aeromagnetic survey was used. A brief description of the different types of filters including the results of their application to the data is further described in the supplementary material (Item DR1).

For 2D forward modeling purposes, we utilized the GM-SYS module in Oasis Montaj, software developed by Geosoft Inc. Three key profiles were selected to cover all the major crustal blocks (Figure 2): (1) a northern profile to study the Esmeraldas and Naranjal blocks, (2) a central profile across the Santa Lorenzo and Piñón blocks to study the highest Bouguer gravity anomaly observed in the region (Figure 3), and (3) a southern profile, coincident with a narrow strip of the high-resolution magnetic data, to study the suture of the accreted sliver across the Gulf of Guayaquil area.

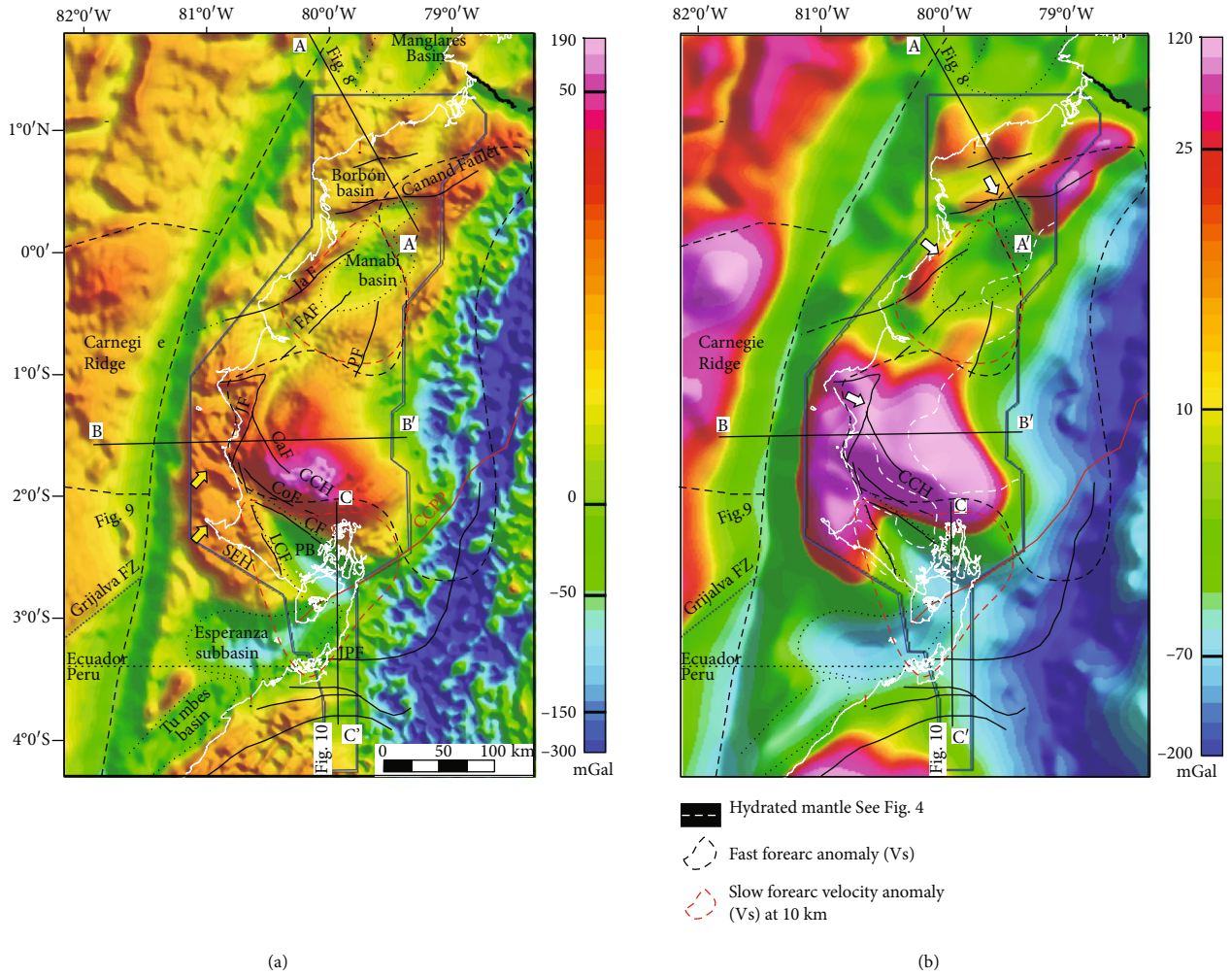

FIGURE 3: (a) A combined Bouguer gravity anomaly map, including satellite gravity data [108] outside the outline of the aeromagnetic survey, marked in blue. At ca. 2°S, a very high positive anomaly is coincident with the Chongón-Colonche hills (CCH). Negative Bouguer's values to the east are associated with a deep Andean crustal root. To the west of the trench, another high positive anomaly is associated with the oceanic Carnegie Ridge. (b) Upward continuation of 10km to highlight the deeper sources of anomalies. Continuous lines in black consist of the compilation of surface faults [30], and the red line represents the CCPP fault system, which is associated with a sharp boundary between the NAS and the Subandean domain overthrusting the SAP [67]. Abbreviations are as follows: CF: Carrizal fault; CaF: Cascol fault; CoF: Colonche fault; FAF: Flavio Alfaro fault; JF: Jipijapa fault; JaF: Jama fault; JPF: Jubones-Peltetec fault; LCF: La Cruz fault; MA: Mulaute anomaly; PB: Progreso basin; PF: Pichincha fault; SEH: Santa Elena High. Dashed black lines represent fast forearc velocities at depth of 20 km, and the red dashed lines slow forearc velocities at depth of 10 km [56].

4.2. Data Constraints for 2D Forward Models. The geometry of the 2D crustal models across the forearc region in Ecuador was mainly constrained by means of existing velocity models and deep and conventional seismic profiles. The properties of the different blocks to initiate the forward models were derived from velocity analyses, paleomagnetism studies, and borehole data (Table 1).

The densities for basement rocks are derived from the velocity analysis of wide-angle seismic data [47, 49, 56], using empirical velocity-density relationships for igneous rocks [60]. For the sedimentary cover, densities were estimated from industrial borehole logs, located in the Gulf of Guayaquil and the Progreso basins. The different densities used in this study are listed in Table 2.

We define the acoustic basement as the Cretaceous oceanic crust underlying the coastal forearc region. Overlying sedimentary packages were roughly averaged with a seismic velocity of 2.3 km/s, to depth convert the top of the acoustic basement. The results of the seismic interpretation of deep and conventional seismic profiles ([46, 49, 56, 61, 62]; and this work) were used to constrain the forearc basement structural configuration as input geometry for the 2D forward models.

Magnetic susceptibility and remanent magnetization values from outcrops along the Chongón-Colonche Hills [20] were used as input parameters for the Cretaceous blocks in our forward magnetic models. For the characterization of the subducting Nazca Plate, natural remanent magnetization

Table 1: Model constraints.

Element to be constrained	Parameter of constraint	Reference
Tectonic settings	Fieldwork and geophysical studies	This work. Aizprua et al. [4]; Bethoux et al. [50]; Calahorrano et al. [46]; Feininger and Seguin [15], Font et al. [51]; Gutscher et al. [52]; Graindorge et al. [49]; Gailler et al. [53]; Hernández et al. [45]; Jaillard et al. [54]; Koch et al. [55]; Luzieux et al. [10]; Lynner et al. [56]; Michaud et al. [57]; Vallejo et al. [8]; Witt and Bourgois [58]
Ecuadorian trench	Bathymetry	SRTM30 plus v7
Subduction slab geometry	Wide-azimuth seismic, OBS	Gailler et al. [53]; Graindorge et al. [49]
Density	Density from seismic velocity profiles	Calahorrano et al. [46]; Gailler et al. [53]; Sanclemente [59]
Magnetic properties	Paleomagnetic studies	Roperch et al. [11]; Luzieux et al. [10]

Table 2: List of parameters used for forward modeling purposes.

(a)

Initial parameter	
Earth's magnetic field (December 2011)	
Magnitude (A m^{-1})	29407 nT
Inclination (deg)	20.58°
Declination (deg)	-0.78°

(b)

Block's name	Density (kg m^{-3})	Susceptibility (SI)	Remanence magnetization		
			Intensity (A m^{-1})	Inclination (deg)	Declination (deg)
Water	1030	—	—	—	—
Piñón	2850	0.01	1.2	-15	50
Hydrated mantle	2900	0.07	—	—	—
Mantle	3300	—	—	—	—
Volcanic arc	2900	0.02	1.4	-15	70
Sedimentary basin	2400	—	—	—	—
Volcano-sedimentary	2700	—	—	—	—

(NRM) values were used from Ocean Drilling Program (ODP) sites 1238 and 1239 [63]. Other blocks were initialized with theoretical values [60], and final parameters were determined based on a best-to-fit approach.

5. Analysis of Regional Geophysical Data

5.1. Seismic, Gravity, and Magnetic Anomalies. The gravity and magnetic data show contrasting anomalies (Figures 3 and 4), which have been grouped into three main geophysical domains based on their different wavelength and textural characteristics.

5.1.1. Outer Domain. A series of short-wavelength Bouguer anomalies and elongated in a NNW-SSE direction characterize the SW coast (yellow arrows, Figure 3(a)). This region is coincident with the Santa Elena block and bounds the Progreso basin to the east. The short-wavelength characteristic of the anomalies extends north, but in an irregular pattern (Figure 3(a)). The eastern boundary of this domain is defined by a high positive and elongated anomaly, which appears segmented and apparently rotated clockwise to the north. This last lineament is also highlighted by a series of elongated magnetic anomalies (Figure 4(a)). An analytical filter applied to the total intensity magnetic map highlights a series of positive anomalies (M1, M2, and M3 sections in Figure 4(b)) of similar textural characteristics. The analytical signal highlights the outline of the possible sources of these anomalies with their eastern edges coincident with the major Jipijapa, Jama, and Canandé faults (Figure 4(b)), a set called here the Coastal Range Fault System (Figure 4). The same textural characteristic appears to extend southwards into the SEH but shifting to a NW-SE direction. This lineament is coincident with the La Cruz fault, delimiting the outer domain from the Progreso basin. From south to north, this lineament, which appears related to a deep source as shown by Figure 3(b), has a concave shape and delimits the outer domain from the inner domain to the east. As mentioned above, this lineament is coincident with major faults and bounds Cenozoic forearc depocenters located landwards

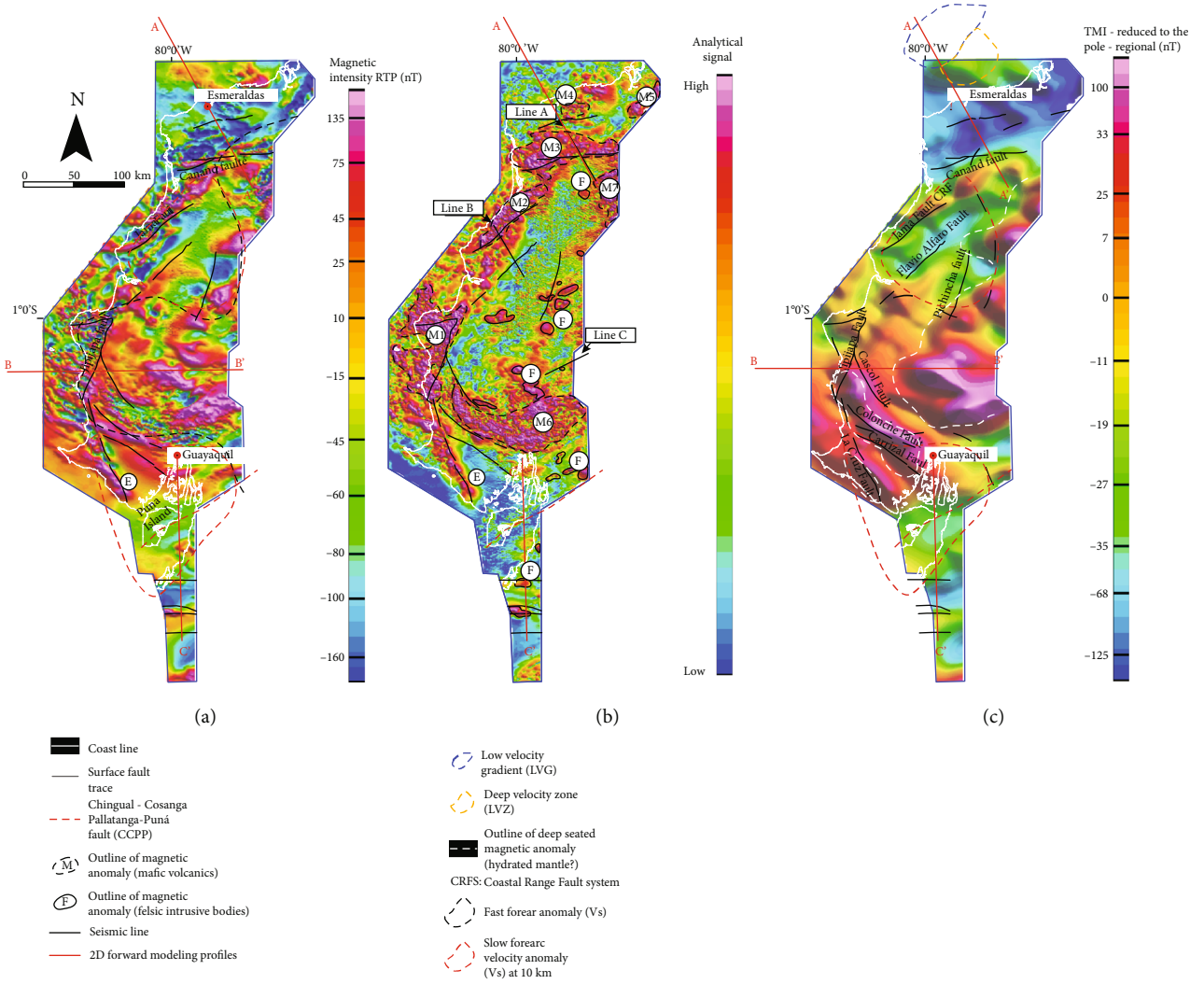

FIGURE 4: (a) Total magnetic intensity (TMI) map-reduced to the pole (RTP) of the forearc region in Ecuador. (b) Analytical signal of the TMI in (a). (c) Upward continuation (10 km) of the TMI in (a). M-type anomalies are associated with mafic-derived bodies, whereas F-type anomaly relates to felsic intrusive bodies. The E anomaly refers to the Estancia Magnetic high, possibly a M-type anomaly and prominent feature in southern Ecuador coincident with the La Cruz fault.

within the inner domain. The unusual feature (E in Figure 4), here termed the Estancia magnetic high, strongly correlates with the La Cruz fault. The Estancia magnetic high (70 nT) suggests that it may be underlain by mafic rocks, presumably from the Piñón formation. Farther south into the Santa Elena High and towards the Puná island, the magnetic intensity has a different anomaly pattern (Figure 4), possibly suggesting the transition into the Santa Elena accretionary complex [4].

The M1 and M2 anomalies highlighted by the analytical signal are characterized by a discontinuity that correlates to the jump between the Jipijapa and Jama faults (Figure 4(b)). Northward into the M3 anomaly, similar textural patterns are observed with its eastern limit apparently rotated in relation to the same structural trends, the Jipijapa and Jama faults, observed to the south. The near E-W orientation of the eastern limit of the M3 anomaly coincides with the Canandé fault, a major bounding fault to the Cenozoic Manabí basin and boundary between inner and outer domains (Figure 4).

The apparent relationship between the eastern limit of the M1 to M3 anomalies to the major bounding faults suggests that the mafic-associated anomalies may partly control the location of major fault activity, possibly as a rheological factor. A close-up look into the transitional region between M2 and M3 anomalies shows the structural complexity of the area and how this may correlate with exposures of the Esmeraldas block and possibly with the southern extent of the Naranjal block (Item DR2). An industrial seismic profile across this area (Figure 5(a)) shows the Canandé fault separating a major structural high to the north from a sedimentary basin to the south. The closely spaced normal faults affecting the top of the basement can be correlated with the geophysical lineaments derived from the analytical signal (Item DR2). A seismic profile farther south (Figure 5(b)) shows similar characteristics to the profile described above

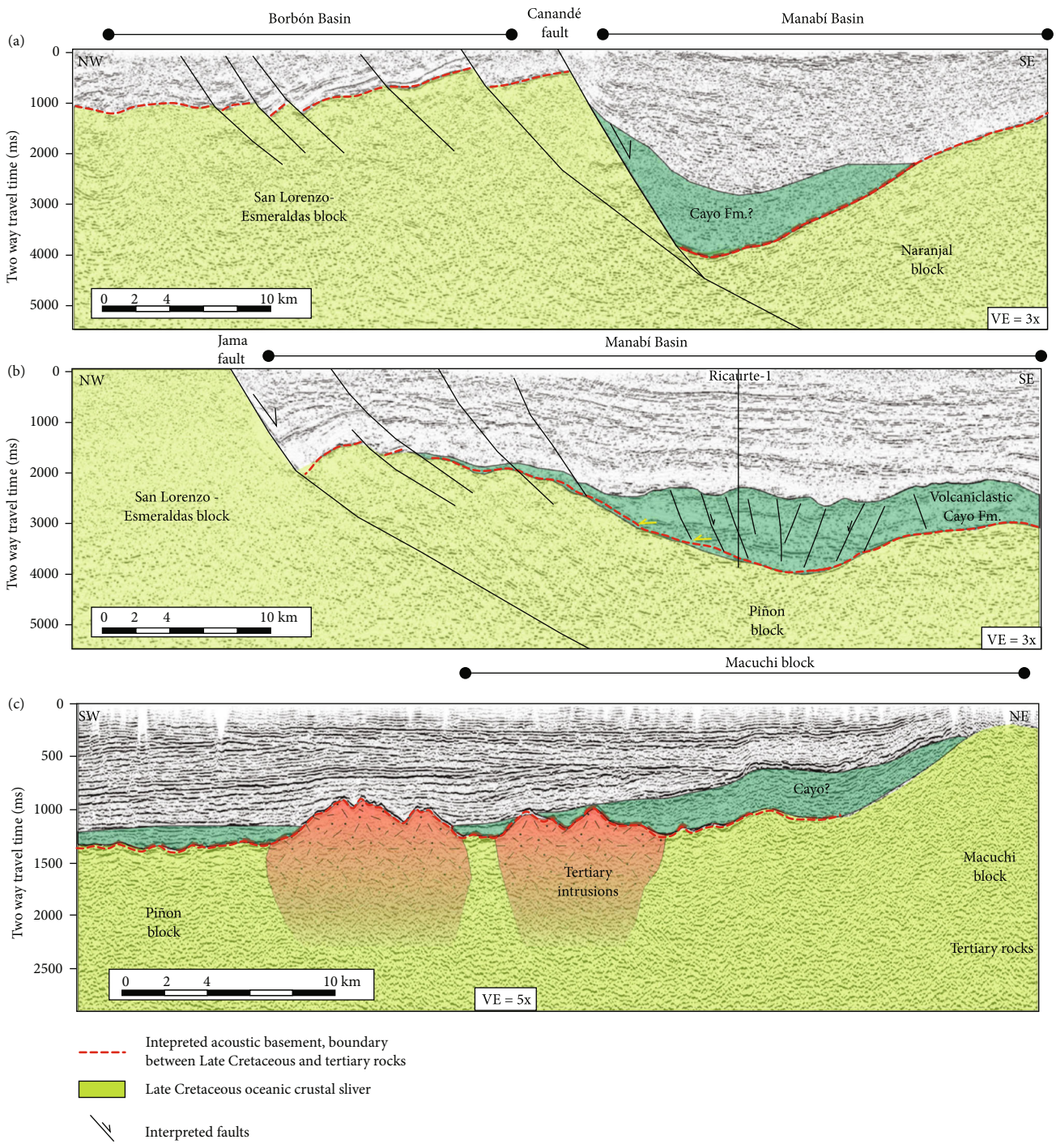

FIGURE 5: Onshore seismic profiles across the San Lorenzo-Esmeraldas and Piñón blocks. (a) A NW-SE profile which shows a series or normal faults dipping landwards west of the major Canande fault, which bounds the Cenozoic Manabí basin. (b) A NW-SE profile showing to the west an uplifted area related to the Cretaceous acoustic basement, and to the east a depocenter possibly underlie by a deformed basement. (c) A NE-SE seismic profile shows an uplifted area towards the north, which corresponds to the exposed Macuchi block. Notice the inferred presence of intrusive bodies possibly emplaced at different ages. Location of seismic profiles in Figure 2.

suggesting that the Canandé and Jama faults delimit the outer domain landwards and may be of a similar origin.

The M4 anomaly, located farther north, appears to have similar textural characteristics in the analytical signal as those observed for M3, however with a less considerable size (Item DR2). The location of the M4 anomaly is coincident with exposures across the structural high called "Businga dome," where rocks of the Late Cretaceous Piñón Formation have been described in the past [30, 64].

5.1.2. Inner Domain. In contrast to the outer domain, the inner domain is mostly characterized by long-wavelength anomalies (Figures 3 and 4). It is limited to the west by the convex-shaped lineament forming the eastern boundary of the outer domain (Figure 3), to the east by the limit of the survey (i.e., Andean piedmont and related outcrops of the Macuchi block), and to the north by the Canandé fault. This domain accounts for a large portion of the forearc region in Ecuador. A key feature of this domain is the high positive amplitude and long-wavelength Bouguer gravity anomaly, coincident with the exposures along the Chongón-Colonche Hills (Figure 3(a)).

From the inner and towards the outer domain, gravity values decrease considerably reaching up to ca. -10 mGal to the north and ca. -50 mGal south of the Chongón-Colonche Hills (Figure 3). The northernmost gravity low within this domain is associated with the Manabí sedimentary basin, which has an elliptical shape with a NE-SW oriented axis.

The analytical signal of the total magnetic intensity anomaly map (Figure 4) shows two major mafic-associated anomalies (M6 and M7). In between these two anomalies, there are a series of patchy circular to elliptical anomalies possibly associated with felsic intrusions, of similar dimensions as those outcropping farther to the east within the Macuchi block (Figure 2). It is likely that the circular anomalies observed in the analytical signal may represent a SW prolongation of the intrusive bodies related to the Macuchi Unit. A seismic profile across this region (Figure 5(c)) shows a localized and irregular acoustic basement relief, typical of igneous intrusions.

The elongated M6 anomaly apparently expanding from west towards the east, exposed along the Chongón Colonche Hills, accounts primarily for rocks of mafic characteristics [10, 19]. Goossens and Rose [31] have previously reported elongated magnetic anomalies located along the Chongón-Colonche Hills, with a predominantly E-W orientation, and associated them with basaltic lava flows. In contrast, in the northern part of the inner domain near the transition to the Naranjal block, the M7 anomaly coincides well with the exposures that define the Naranjal block (Item DR2), suggesting that the anomaly may be a southward prolongation of the former.

5.1.3. Southern Suture Domain (Gulf of Guayaquil). The positive Bouguer gravity anomaly over the Santa Elena block decreases to the south where it becomes negative over the Esperanza subbasin (Figure 3(a)). A rapid change related to the thick sedimentary succession of Quaternary deposits in the Esperanza subbasin, a depocenter that is associated with the northward migration of the North Andean Sliver [4, 65], whereas along the Tumbes basin, the gravity low is likely to be controlled by a s.s. forearc depocenter [4, 66]. Across the Ecuador-Peru border, south of the Tumbes basin (Figure 3), the gravity anomaly increases towards the Amotape-Tahuin Massif, which is of continental affinity and marks the southern limit of the suture domain.

The gravity map shown in Figure 3(a) shows an apparent oblique relationship between the Tumbes and Esperanza gravity lows. From the Esperanza subbasin towards the continent, the gravity low area narrows drastically into a location where it coincides with the major Chingual-Cosanga-Pallatanga-Puná (CCPP) fault system defined by Alvarado et al. [67] (Figure 3(a)). The wider part of the whole negative anomaly may be associated with (1) the possibly northward displacement of the Santa Elena High, which is part of the North Andean Sliver tectonic scape [4], or (2) the trenchward extension of the Jubones fault. The latest is the southernmost location of the suture between the accreted oceanic terranes of the CLIP and the continent. At the narrow section of the gravity low, Late Cretaceous rocks from the Pallatanga Formation (an age equivalent to the Piñón Formation) are interpreted to underlay the sedimentary basin in this region [4].

Despite only partial coverage of the aeromagnetic survey across the eastern part of the Gulf of Guayaquil, this has allowed us to better constrain the deep crustal structure across a major boundary (Item DR2). The magnetic intensity map-reduced to the pole (RTP) shown in Figure 4(a) shows a decrease of values over the Puná island, pointing towards a reduction in magnetic susceptibility of the region. The disposal of the magnetic anomalies, shown in Figure 4(a), appears to correlate with some surface exposure of crustal units in the area. For instance, south of the Puná island, a prominent magnetic source correlates with the strike of the ultramafic Raspas Complex, an exhumed fragment from a Late Jurassic-Early Cretaceous subduction system [34, 68]. This magnetic high is bounded to the north by a magnetic low striking E-W and coincident with the trend of the Jubones fault (the southernmost identified suture) and to the south by the Late Cretaceous Lancones sedimentary basin.

5.2. Forward Models

5.2.1. Crustal Structure. Overall the model A-A' shows an average thickness of 15 km of crust (Figure 6(c)), based on a best-fit approach, with some variations at the different domains. At the outer domain in profiles A-A' and B-B' (Figures 6 and 7, respectively) the seaward decrease of the gravity anomaly may be indicative of thickness or density variations. For instance, at profile A-A' (between 20 and 50 km, 2600 kg/m^3), this lower gravity anomaly may be associated with a low-velocity zone along the western part of the prestacked depth migrated SIS-line 44 presented by Collot et al. [62], who suggest that this block represents an altered outer wedge affected by deep-sourced fluids flowing along crustal faults. Indeed, a three-dimensional velocity model covering the same block [61] supports a low-velocity zone that may be related to altered and hydrated mafic and ultramafic rocks, commonly observed along margins consisting of oceanic or island arcs accreted terranes. Furthermore, recent tomography-based shear velocity inversion models reveal low-velocity crustal bodies possibly associated with the subduction of the Carnegie Ridge, north of 1°S (Figure 3) [55, 56]. East of the low-density zone (Figures 6(b) and 6(c)), a high-amplitude magnetic anomaly shows decreasing values towards the Borbón basin. The magnetic contrast towards the east (0.01 SI) extends from 60 to 110 km in profile A-A'. In between 110 and 140 km, both the magnetic and

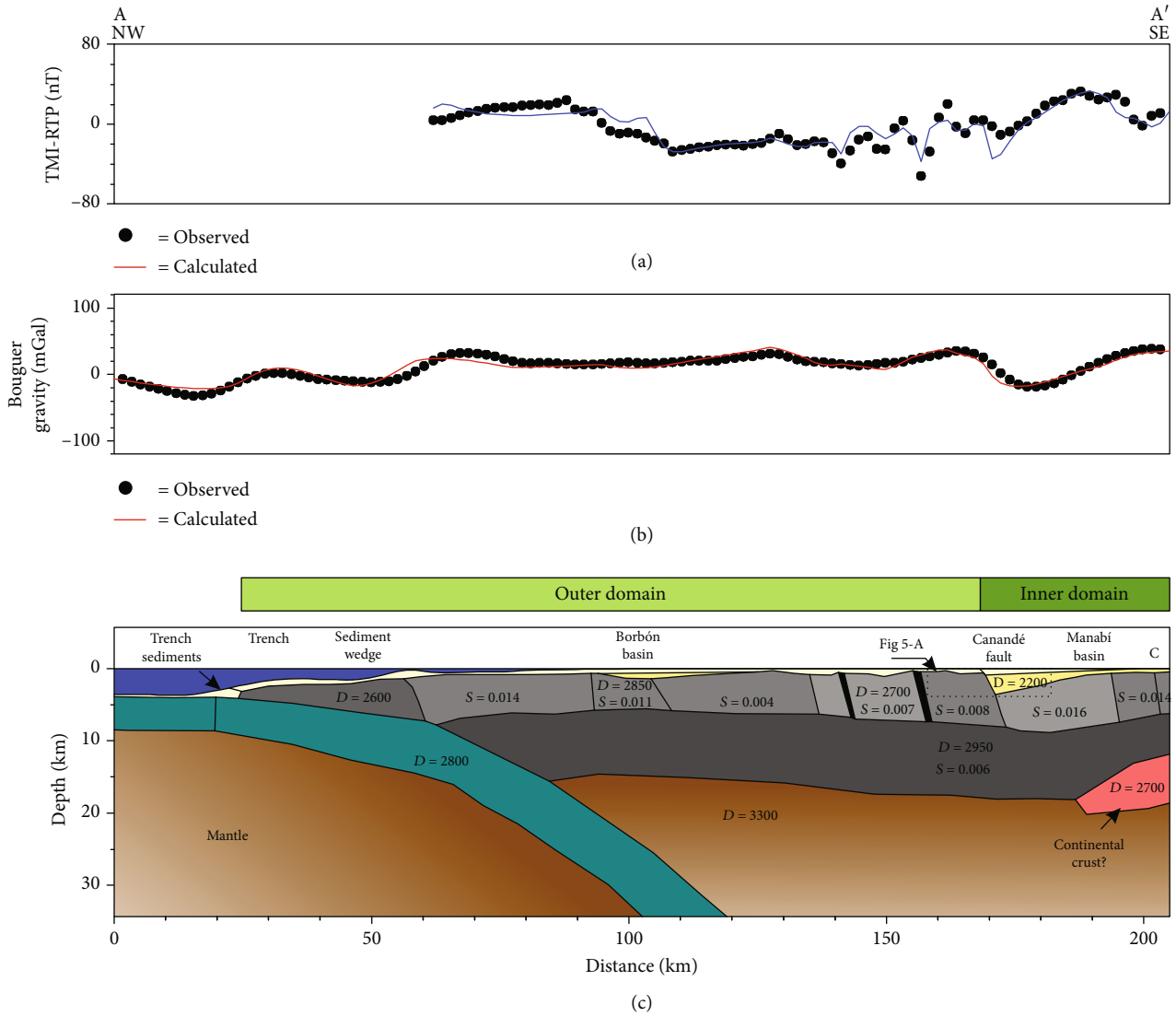

FIGURE 6: Two-dimensional gravity and magnetic forward models along profile A-A', between 2°N and 0°. (a) Observed and calculated total magnetic intensity reduced to the pole (TMI-RTP) across the profile, using the international geomagnetic reference field (IGRF) as the initial parameter listed in Table 1. (b) Bouguer's gravity observed and calculated anomaly showing very small differences. (c) Geological cross-section with the different blocks constrained by surface geology and deep seismic profiles.

gravity anomalies are characterized by a flat gradient prior to entering into an area of varying magnetic values, associated with the major Canandé fault zone, as observed on the seismic profile shown in Figure 5(a). A series of faulted blocks with varying magnetic susceptibility are added to match the varying magnetic profile west of the Canandé extensional fault (Figure 6(a)). The blocks are vertically extended from the inferred top basement down to depths of 7-9 km matching the upper boundary of a higher density (2950 kg/m^3) and laterally extended lower crust. The inferred fault system may be also associated with NNE-SSW dyke-shape mafic bodies, considering the high degree of variability in the total magnetic intensity map, a typical response encountered at low latitudes [69]. The Canandé fault also marks the base of a steep gravity gradient and the eastern edge of the irregular magnetic zone. In our model, the depocenter of the Cenozoic Manabí basin and a less dense Late Cretaceous oceanic crust basement account for this steep gradient marking the boundary between the inner and outer domains.

Along profile B-B', anomalies are matched with a relatively shallow Moho with ~10 km depth and up to 15 km depth towards the Andean piedmont (Figure 7). The gravity anomaly and derived model show a similar pattern towards the trench as in A-A', except that values are considerably higher compared to profile A-A'. To fit the anomaly, across the outer domain, a thicker upper crustal block (of ca. 7 km) with a density of 2740 kg/m^{3}was adjusted into the model. This thicker upper crustal unit appears to relate to an outer-wedge geometry in the west, which may partly correspond to the northern prolongation of the interpreted Santa Elena High farther south. The latest consists of thick and highly deformed successions of Late Cretaceous to Paleocene sediments [4, 21, 46]. The highly deformed nature of the Late Cretaceous and Paleocene series of the Santa

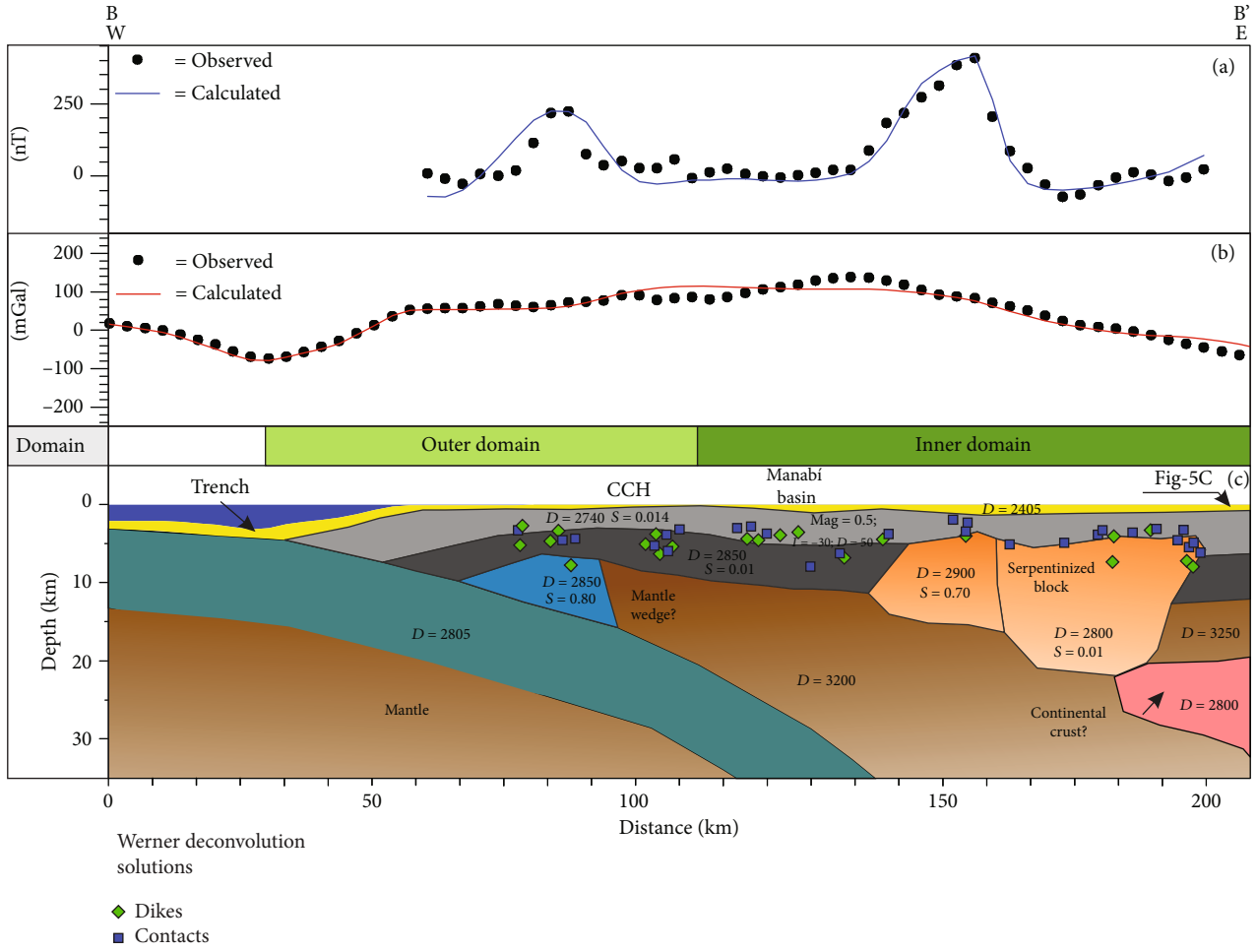

FIGURE 7: Two-dimensional gravity and magnetic forward models along profile B-B', between 1° and 2°S. (a) Observed and calculated total magnetic intensity reduced to the pole (TMI-RTP) across the profile, using the international geomagnetic reference field (IGRF) as the initial parameter listed in Table 1. (b) Bouguer's gravity observed and calculated anomaly showing very small differences. (c) Geological cross-section with the different blocks constrained by surface geology and deep seismic profiles [49, 56]. Density values are shown in the section, and magnetic susceptibility and remanence are listed in Table 1.

Elena block and the tectonic interaction with the Piñón block (here, the inner domain), this last one acting as a backstop [4], support this outer-wedge model (Figure 7).

The spectral analysis of the total magnetic intensity map indicates that the magnetic anomalies within the inner domain may be originated at different depth levels (Figure 4 and Item DR1). An initial model test with magnetized bodies at medium to shallow depth (<10 km) and susceptibility values between 0.01 and 0.02 SI account partly for the observed magnetic anomalies within the inner domain in profile B-B' (Item DR3). An alternative interpretation for this initial model may include faults; however, it still requires the presence of highly magnetized bodies. We do not rule out a combined model, where highly magnetic bodies are associated with deep-seated faults.

The long-wavelength component of the magnetic anomaly has been modeled considering deeper sources, to a depth of 10-15 km (Figure 7). Two different scenarios were considered to match the main gravity low in the east part of the model. The first scenario involves a low-density polygon located at the base of the oceanic crust representing a fragment of the continental autochthonous crust; a low-density polygon is necessary in order to match the gravity low without reaching an anomalous high thickness for the accreted plateau rocks. The second scenario (Figure 7) involves a similar autochthonous polygon with a paleohydrated mantle wedge necessary to match the high positive magnetic anomaly. This last scenario is the preferred one, together with the presence of continental crust, as supported by the velocity model presented by Lynner et al. [56]. Indeed, partial serpentinization of the lower crust or a remnant hydrated mantle wedge may be the source of the positive magnetic and negative gravity anomaly pair (see next section). The magnetic anomaly to the west in profile B-B' (between 80 and 110 km, Figure 7) is located near to a high to low shear velocity zone according to the model proposed by Lynner et al. [56] (Figure 4). Considering the gravity decrease in this area, the presence of magnetic underplated material or a hydrated mantle wedge seems plausible models. Similar observations are reported across other active margins, with the presence

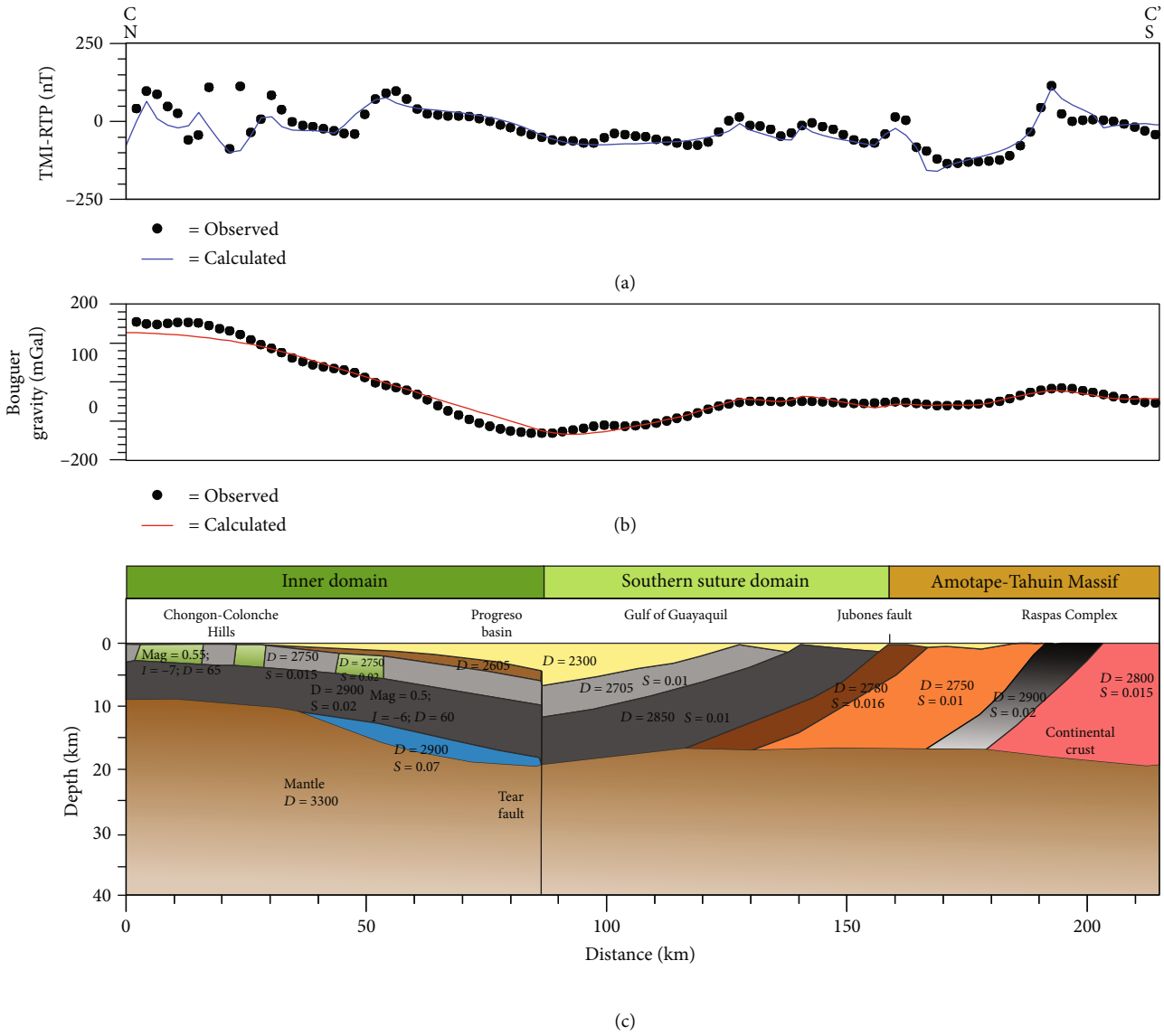

FIGURE 8: Two-dimensional gravity and magnetic forward models along profile C-C', between 2° and 4°S. (a) Observed and calculated total magnetic intensity (TMI) across the profile, using initial parameters listed in Table 1. (b) Bouguer's gravity observed and calculated anomaly. (c) Geological cross-section with the different blocks constrained by surface geology and seismic profiles. Density and magnetic susceptibility are shown in the section.

of a hydrated mantle wedge underlying a forearc basement of oceanic affinity like in Oregon and East Antarctica [70, 71].

5.2.2. Southern Suture of the North Andean Sliver to the Continent. To investigate the southern suture between the trapped oceanic sliver and the continental South American Plate, we have integrated the observed tectonic elements of the area and modeled the gravity and magnetic response along profile C-C' (see Figure 2 for location). The northernmost segment of profile C-C' (Figure 8) partly crosses the eastern extent of the Chongón-Colonche Hills, which are characterized by surface exposures of the Piñón Formation and by the highest gravity anomaly in the region discussed in the previous section (Figure 3(a)). The high-amplitude gravity anomaly decreases towards the center of the profile and coincides with the southeastern extent of the Progreso basin (Figure 8). This segment crosses a series of high-magnetic anomalies that were matched by introducing shallow bodies (0.01 SI) and a deeper source of high magnetic susceptibility (0.07 SI) extending to a depth of ca. 15 km comparable to profile B-B'.

Towards the south, at the Gulf of Guayaquil (Figure 8), the gravity anomaly drops to a minimum of ca. -120 mGal. A strong lateral contrast in density coincident with the base of the steep gravity gradient was introduced in the model to account for this gradient. Although less constrained than profiles A-A' or B-B', the profile C-C'could be divided and analyzed into two main segments: (1) the northern segment characterized by high gravity values as well as long-wavelength magnetic anomalies that extend laterally along

the Chongón-Colonche Hills (Figure 4) and (2) the southern segment presenting a gentle southward stepping-uptrend of gravity values and lower magnetic contrasts. In between 90 and 125 km (Figure 8), gravity values increase to ca. -60 mGal staying almost constant up to 180 km, where it increases again up to -20 mGal. At the lowermost gravity point (at ca. 90 km), the SE extend and deepening of the Progreso basin connects to the eastern extent of the Gulf of Guayaquil basin, without any hint on the eastward presence or continuation of the Santa Elena High, as described by Aizprua et al. [4] (Figure 8).

A series of north stepping magnetic highs, in between 120 and 210 km, characterized by steep slopes to the north and gentle gradients to the south (Figure 8) are modeled by a stacked series of blocks probably developed during the Late Cretaceous accretionary phase, later reactivated by extensional tectonics. Large basement faults with an extensional component have been previously reported in this area based on seismic profiles [4, 65, 72]. The southernmost part of the model is constrained by the surface exposure from the Raspas Complex that coincides remarkably well with a high magnetic peak (at ca. 190 km) and the slight increase in gravity values forming a bell-shaped geometry. In between this area and the Jubones fault (Figure 8), the model is fitted with a block of lower density (2750 kg/m^3) comparable to the block south of the Raspas Complex, suggesting that this area might be considered the continuation of the NE of the metasediments from the Amotape-Tahuin Massif or it consists of a transitional zone to the obducted oceanic section (Figure 8).

6. Discussion

The gravimetric and magnetic anomalies in the Ecuadorian forearc show a clear correlation to the crustal exposures across the coastal region. Furthermore, the structural interpretation based on the anomaly's gradients correlates well with their surface expression allowing to extend the interpretation to buried areas. The compilation of the different lineaments interpreted from the spectral analysis of gravity and magnetic anomalies provides clear evidence of a complex crustal architecture (Figure 9), most likely inherited from the Late Cretaceous allochthonous terranes (CLIP)-passive margin collision event.

It is admissible to conceive that the structure of the current Ecuadorian forearc and part of the arc will depend on the preservation degree of the accreted terranes during the arc-continent collision, which is controlled at the first order by the polarity of subduction [12]. A major discrepancy in the precollision settings of the Late Cretaceous arc is related to the subduction polarity. A west-dipping subduction system colliding perpendicular with the South American margin, presented by Vallejo et al. [8], is in accordance with the "forward-facing" arc-continent collision type-1 (the forearc collides first) proposed by Draut and Clift [12], which may lead to the preferential preservation of the intraoceanic arc, as observed in the northern part of the Western Cordillera. Suggested evidence for a westward polarity includes regional models proposed for volcanic island arcs located in Colombia and farther north in the Caribbean region and the absence of magmatism older than 85-80 Ma in the Ecuadorian margin [8]. Nevertheless, alternative models based on tomography and supported by a quantitative plate reconstruction support an east-dipping subduction system in the Northern Andes [1, 9]; a similar polarity has been considered in models across western Ecuador, inferred from a geochemical and stratigraphic approach (e.g. [5–7]). Suggested evidence for an eastward subduction includes the lack of a clear magmatic gap from the older oceanic plateau lavas (Piñón Fm.) to younger arc lavas, expected during a polarity reversal as proposed by Vallejo et al. [8]. Collision with an eastward polarity is in accordance with the "backward-facing" arc-continent collision type-1 (the back-arc collides first) proposed by Draut and Clift [12], which may lead to the preferential loss of the back-arc system.

6.1. Split of Rio Cala-San Lorenzo Arc and Development of a Marginal Basin? Major block rotation that took place between 70 and 75 Ma probably triggered the initial crustal fragmentation of the forearc area [10]. The series of high magnetic susceptibility sources along the outer domain (Figure 4(b)) appear to correlate with plateau and island arc-associated formations described within the San Lorenzo block (Figure 2) [7, 10]. The coincidental location of the major faults bounding the eastern limit of the M1, M2, and M3 anomalies (the Coastal Range Fault System, see Figure 4) suggests rheological controls on the formation of this major boundary. The patchy and apparent northward change in orientation between the M2 and M3 anomalies, along the Canandé fault, suggests crustal deformation possibly accompanied by block rotation. In addition, the lack of continuity between M1 and M2 anomalies (Figure 4) could be explained by a fault-related demagnetization process following block fragmentation and strike-slip movements. This area is coincident with the development of the Pedernales basin [45, 73] within the outer domain.

Both the San Lorenzo and Esmeraldas blocks are characterized by the presence of volcanic rocks from the San Lorenzo Formation unconformably overlain by middle Eocene rocks, marking a clear stratigraphic hiatus [74]. A stratigraphic gap supports the interpretation of a structural high developed by Late Cretaceous [10, 75, 76]. Furthermore, an oil exploratory well located in the inner domain (Ricaurte-1 in Figure 5) encountered (near its bottom) a series of volcaniclastic deposits (Coniacian to Campanian) that correlate to the Cayo Formation described farther south along the Chongón Colonche Hills [72, 74, 77]. The on lapping stratal termination pattern of the lowermost seismic unit onto the Piñón acoustic basement suggests that the depocenter and the bounding structural high were coeval with the sedimentation of the Cayo Formation. Thus, the onset of sedimentation in the Cayo Formation may have preceded the main accretion whereas the upper part is synchronous with the major tectonic event during Late Campanian characterized by clockwise block rotations, between 75 and 70 Ma, recorded by paleomagnetic declination [10, 11] and most likely associated with the main Late Cretaceous accretionary period in Ecuador [6–8]. Although the temporal relationships between the San Lorenzo and Rio Cala arcs are poorly constrained

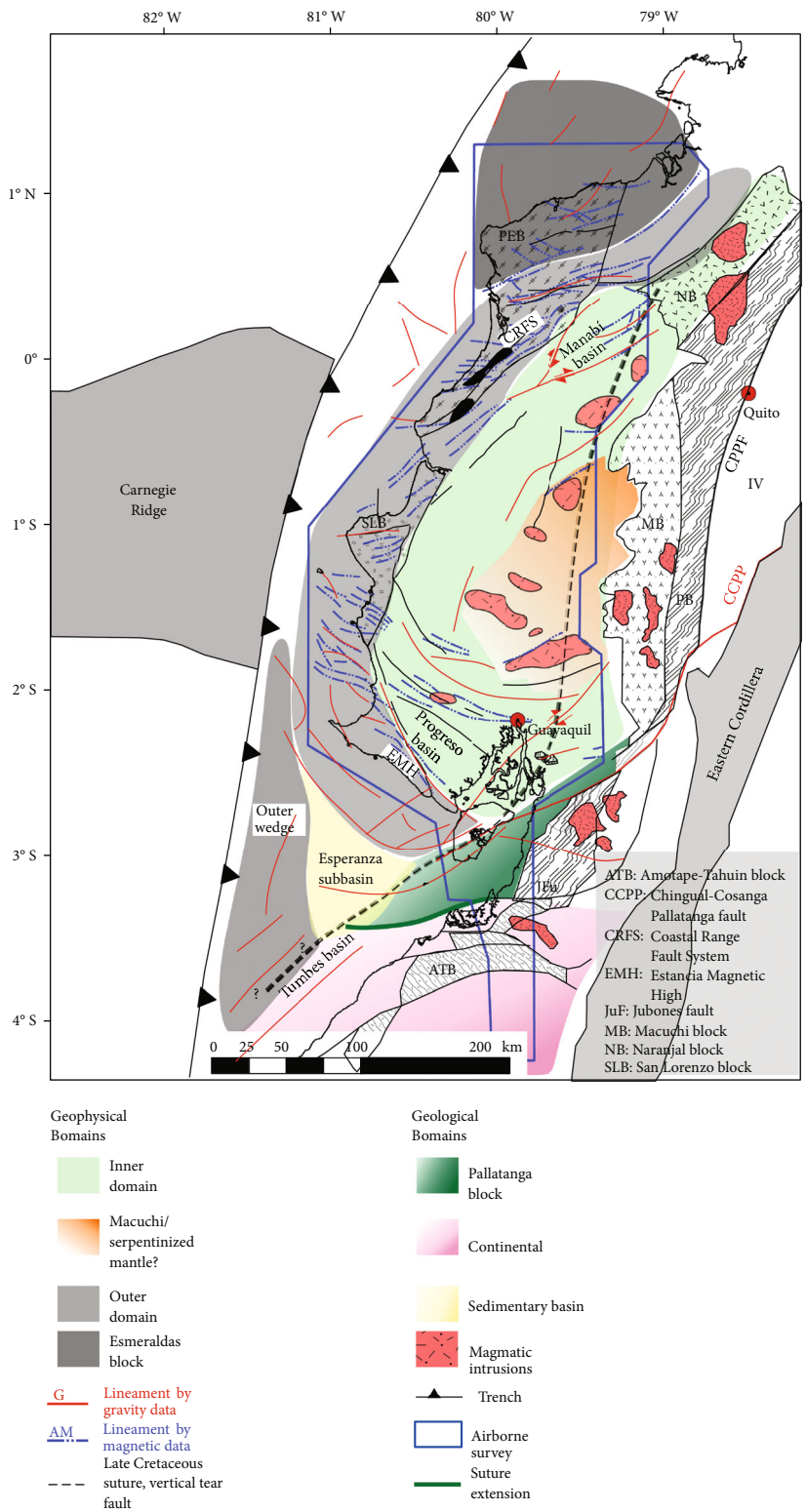

FIGURE 9: Crustal model of the Western Ecuador forearc region depicting the different geophysical domains and buried elements derived from the interpretation of combined gravity and aeromagnetic data.

(especially because of poorly defined ages for the Rio Cala arc; see [8]) the wealth of observations suggests that the outer domain and more specifically the San Lorenzo arc may represent the western section of a split arc. An early separation between these two arcs may have developed a marginal Late Cretaceous basin, where sedimentation of volcaniclastic deposits of the Cayo Formation took place. It is, however, difficult to conceive the mechanism leading to the formation of

the marginal basin, especially because of doubts about the temporal relationships between the arcs and the subduction polarity during Late Cretaceous. However, the very weak deformation observed at the base of the depocenter, interpreted here as a marginal basin, suggests that the accreted sliver was most likely transferred to the continental margin with little internal deformation. This last aspect may be interpreted as a highly preserved sliver because of forward-facing collision. Nevertheless, a weak deformation may also be conceivable in the context of a thick accreted sliver colliding in a backward-facing mode and even with a transcurrent accretion mode.

At the southernmost part of the inner domain, we found one of the most significant positive and long-wavelength Bouguer anomalies in the northern Andes located along the Chongón Colonche Hills. Feininger and Seguin [15] and this study estimate that a shallow mantle and a thinner crust (down to 7 km locally) are contributing to the anomaly. This may be considered atypical for an oceanic plateau or for an island-arc, as they commonly exhibit thicknesses above 10 km [78]. Recent studies based on seismic tomography put in evidence a high shear velocity zone that correlated very well with this gravity anomaly, confirming the shallow mantle model (Figure 3). Indeed, farther north, the thickness of the accreted sliver increases and reach values of ca. 15 km (Figure 6). The very significant positive anomaly seems coincident in the southern limit of the marginal basin, here related to a possible split of the Rio Cala and San Lorenzo arcs. Therefore, crustal thinning and resulting isostatic mantle upwelling may well explain this gravity high in the region. Additionally, preliminary petrological analysis on intrusive rocks at the eastern part of the CCH [79] suggests significant denudation in excess of 2-3 km subsequent to the magmatic activity. Nevertheless, this hypothesis needs further verification, especially regarding the timing of the denudation period and its relationship with better known rotational and accretional periods in SW Ecuador.

6.1.1. The Regional Positive Magnetic Anomaly: A Serpentinized Mantle? We propose that a combination of (1) deep-seated faults controlling basalt flow location and (2) disturbances of the underlying mantle possibly through a serpentinization process may have considerably modified the density and magnetic properties of the underlying forearc basement or crustal mantle.

It is widely accepted that at depths of ~40-50 km, the subducting slab releases large amounts of water into the overlying lithosphere producing serpentine [70, 80]. Serpentinization can be distributed extensively affecting in some cases the entire forearc mantle [70]. It is known that serpentinization reduces the density of peridotites and produces a residual iron oxide, typically magnetite, which imparts a strong magnetic susceptibility to serpentinites, where its value is proportional to the degree of serpentinization and amount of iron derived from source rocks [80, 81]. Magnetic susceptibilities may increase by several orders of magnitude; remanent magnetization may increase by one order whereas density may decrease from ~3000 kg/m^3 to ~2500 kg/m^3 (e.g., [70, 82]). Therefore, and as suggested by Blakely et al. [70], long-wavelength magnetic anomalies lacking corresponding positive gravity anomalies may provide evidence to map hydrated mantle in convergent margin settings. Forearc hydrated mantles may also have a strong influence on deformation partitioning and seismicity at depth [83, 84], and they have been usually discovered by the presence of anomalous low velocities in mantle regions (e.g., [70]).

The long-wavelength component of the anomalies described within the inner domain suggests that part of the anomalies may be originated at great depths. Thus, the very high positive magnetic anomaly (~250 nT) observed at ~180 km in profile B-B' is not paired with a positive gravimetric anomaly, although the gravimetric low may be masked by the vicinity of the continental crust. In addition, the presence of small circular anomalies, highlighted by the analytical signal in Figure 4(b), with high magnetic susceptibility may suggest the presence of magnetite-rich igneous intrusions built on the accreted and composite sliver. Indeed, the apparent serpentinization of the forearc mantle does not appear to correlate to the modern arc (actually, a high-velocity mantle has been defined in the area; Lynner et al., 2020), and instead, it may be related to ancient plutonism. We suggest that part of the inner domain underlying the crustal mantle may have undergone a serpentinization process giving rise to this significant magnetic anomaly (Figure 4(c)), most likely coevally with the magmatic intrusions, which east of the piedmont has been dated between 43 and 25 Ma in the Macuchi block [85]. Similar anomaly patterns have been observed along other active margins that share similar characteristics in terms of forearc sliver accretion, like in Cascadia on the Oregon coast [70], East Antarctica [71], and Japan [86].

The Macuchi block, just east of the inner domain, is characterized by a broad volcanic arc region and marked by pulses of adakite-like magmatism [87]. This author attributes the peculiar adakite-like magmas to a process of crustal thickening through the build-up of previous magmatic arcs. Indeed, the hydration of the mantle may have considerably modified the upper crustal structure through the emplacement of volcanism and felsic intrusive material such as the intrusives of the Macuchi block [85, 87–89]. The intrusions observed beneath the forearc depocenter, considered together with coeval intrusions outcropping in the Western Cordillera, may possibly represent the wider magmatic arc of the Cenozoic history of the Northern Andes of Ecuador (Figure 10(b)). In this context, the serpentinization process may have played a significant role in the generation of mineral deposits during Late Eocene to Oligocene such as the porphyry/epithermal Balzapamba, Chazo Juan, and La Plata deposits. Indeed, the suite of porphyry Cu-Au and epithermal Au deposits, such as those encountered in Ecuador, have been related to water-rich, calc-alkaline magmas originated by partial melting of a hydrated mantle wedge (e.g., [90, 91]). Alternative models for the serpentinization within the inner domain may be related to the obduction process of continental crust [92, 93]. Either process may have led to serpentinization of the mantle and lower crust, diminishing the density and therefore a reduction on the gravity anomaly. This may shed

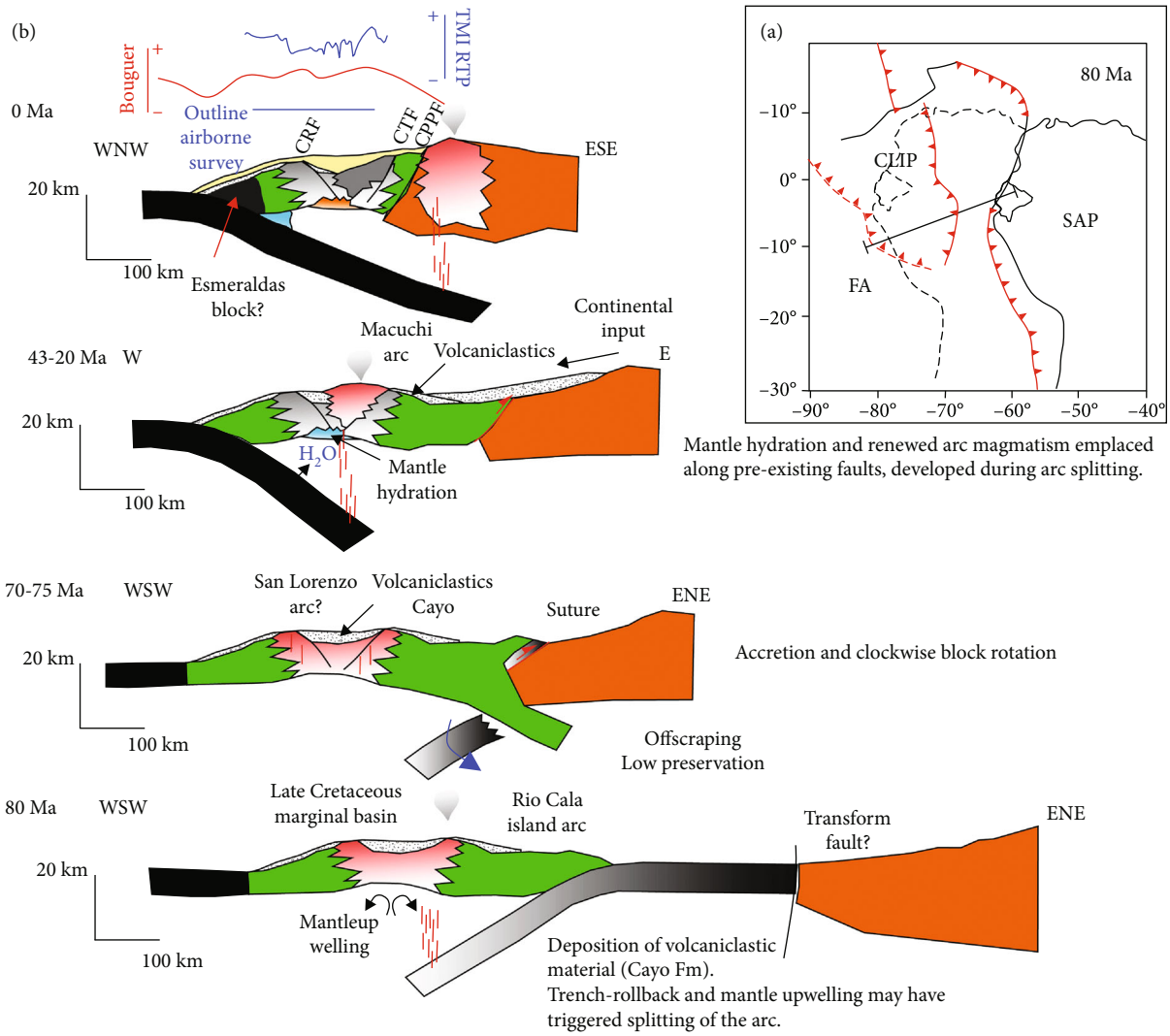

Figure 10: Geodynamic model of the oblique collision between the Caribbean Large Igneous Province (CLIP) and the South America passive margin (Western Ecuador). (a) Plate reconstruction at 80 Ma (modified after [9]). (b) Proposed tectonic evolution of the Western Ecuador subduction system showing an initial west-dipping subduction direction [8]. An alternative model is proposed by [6] controlled by an initial east-dipping subduction direction and a transform fault along the continental margin. Both alternatives are shown in (a). Continous red line after [8] and red dashed line after [6]. FA: Farallon Plate; SAP: South American Plate.

some light on the up to now disputable Macuchi event (Late Eocene to Oligocene event) in the Ecuadorian geology.

6.2. Esmeraldas Block: Trailing Edge of a Different Accreted Sliver? South of the city of Esmeraldas, the total magnetic intensity map reveals strong negative anomalies oriented in a NE-SW direction, a pattern that differs from those observed along the outer domain (Figure 4). Figure 4(c) shows a deep source (>10 km) contributing to the negative anomaly. The southern limit of the anomaly coincides with the major Canandé fault. This long-wavelength and negative magnetic anomaly appears to extend trenchwards and landwards to the northeast prolonging into Colombia, where a major strike-slip system and a double forearc basin system have been previously described [76, 94]. The Borbón and Tumaco basins in Ecuador and Colombia, respectively, are coincident with the location of the magnetic low, with major basin development onset by Early Miocene [76]. In Western Ecuador, the set of strike-slip duplex appears limited to the Esmeraldas block and northwards into Colombia. The northern limit of the magnetic low coincides with the southern prolongation of the Buenaventura fault described in Colombia. The latter is interpreted as the suture trace between the Gorgona and the Dagua terrane (equivalent to the Piñón terrane) [95], both of an oceanic plateau origin. However, paleomagnetic data from the Gorgona terrane [96] may suggest a different plateau origin compared to the CLIP [97, 98].

Farther north at the edge of the aeromagnetic survey, a slight increase in magnetic susceptibility appears to coincide very well with a decrease in gravity (Figure 3). Furthermore, the outline of a low-velocity zone, inferred from a tomographic model [61], agrees with the gravity/magnetic relationship described above. This relationship may be attributed to a serpentinization process of mafic rocks, commonly present

along the convergent margin, such as the one described in the present work associated with the Macuchi block, and like those observed in south-central Alaska [99] or western Oregon [70].

Thus, we cannot discard that the Esmeraldas block could be the southern prolongation of a different sliver such as the Gorgona sliver described by Cediel et al. [95], which extends farther north and possibly giving rise to the development of a double forearc basin system as observed in Western Colombia [94].

6.3. The Southern Suture Zone (Gulf of Guayaquil): A Transform Fault Boundary. The southern suture, across the Gulf of Guayaquil, between the oceanic crustal sliver from the CLIP and the South American Plate, remains uncertain giving rise to different interpretations. For instance, Bourgois [100] proposes two end-member tectonic reconstructions for the underlying crustal structure across the Gulf of Guayaquil-Tumbes basin to better explain the movement of the North Andean Sliver through (1) reactivation of ~75-65 Ma ophiolite suture by simple shear or (2) pure shear along the Inter-Andean depression. Onshore, south of the Puná Island, the depression coincides with the Jubones-Peltetec fault (Figure 2). Giving the partial coverage of this area by the airborne survey, we discuss the possible location of the suture based on the forward model presented in Figure 8 and the spatial distribution of the different tectonic elements (Figure 4), which may be inferred as inherited from the underlying crustal configuration.

The forward model along profile C-C' (Figure 8) was geologically constrained based on surface and subsurface observations [4, 68, 100–102]. We consider that the gravity low south of the major long-wavelength gravity high described along the Chongón Colonche Hills may be caused by a great lateral density variation possibly controlled by a major transform fault. Considering that the Gulf of Guayaquil area may be the southernmost region where a west-dipping subduction system from the CLIP interacted with another subduction system along northern Peru (Figure 10(a)), it is plausible that both systems connect through a transform fault as shown by analogue modeling [103]. Fault segments with a possible shear character, such as the Puná segment [67, 104], are apparently rooted in this major transform fault, which is defined as a vertical tear fault.

Farther to the west (Figure 10), there are two key elements to consider for positioning the suture: first, the presence of the Santa Elena High, which consists of deformed Late Cretaceous to Paleocene sequences possibly conforming an outer wedge remnant of an east-dipping subduction system ([4]), and second, the clear oblique relationship between the Tumbes and Esperanza associated gravity lows (Figure 3). This may suggest that the underlying crustal structure across the Tumbes basin differs from the Esperanza subbasin. Indeed, Aizprua et al. [4] and Espurt et al. [66] propose that the Tumbes basin may conform a forearc s.s. basin controlled to the north by the Banco Peru outer forearc high and underlain by the offshore continuation of the continental Amotape-Tahuin Massif.

Forward modeling seems insufficient to define the southern suture zone of the CLIP. Nevertheless, by putting together all the elements, we considered that the suture zone across the Gulf of Guayaquil is composed of both a suture and a vertical tear fault (Figure 8), both inherited from the collision and accretion process during Late Cretaceous, a model composed of elements from both end-members proposed by Bourgois [100].

7. Conclusions

We put forward the first crustal model for the forearc region in Ecuador that integrates spectral analysis of gravity and magnetic data along with 2D forward models and seismic data. It incorporates previous geophysical, geochemical, stratigraphic, and structural observations mostly derived from the ophiolites emplaced along the Western Cordillera and Coastal regions. It is noteworthy that the analyses and interpretation of the geophysical data were tied to geological constraints at least for the shallowest sources of the anomalies. The crustal structure model of an exceptionally well-preserved remnant sliver from the CLIP provides additional constraints when building a geodynamic model for Western Ecuador.

Our model is composed of at least three main geophysical domains, which are (1) the inner domain, (2) the outer domain, and (3) the southern suture domain. The inner and outer domains here defined on the basis of their geophysical characterization may be in direct relationship to the structuring of the forearc basement, possibly prior to the entrapment of a sliver from the CLIP, during the collision and further fragmentation. For instance, the disposal and alignment of the mafic-associated magnetic anomalies (M1 to M3) along the outer domain, bounded to the east by major faults, here defined conjointly as the Coastal Range Fault System, may suppose an underlying rheological control. Furthermore, the presence of Coniacian to Campanian volcaniclastic deposits, within the inner domain, onlapping onto the structural high, delimited by the fault system mentioned above suggests the development of a marginal basin prior to the collision and accretion of the plateau. The post-Oligocene deformation due to an oblique subduction may have resulted in the development of strike-slip systems [4, 30, 58, 105] across the outer domain and thus the disposal and apparent rotation of the outer domain magnetic anomalies.

The presence of a high positive gravity anomaly and 2D forward models support a very shallow Moho in this region with a thin crust atypical of an oceanic plateau and most likely related to the process leading to the split of the San Lorenzo arc.

Another key factor of our interpretation is related to a regional long-wavelength magnetic anomaly across the inner domain, at least in partly pair with a gravity low, which may suggest the presence of an underlying serpentinization process, with intrusions built on the accreted and composite sliver. Based on the irregularities of the magnetic anomaly, the serpentinization process may have altered the lower crust or the mantle crust underlying the CLIP as suggested by

forward modeling. The general disposition of the high magnetized area seems to coincide with the western edge of the exposed Macuchi block, suggesting that the magmatism type present in the block may be at least partly related to the serpentinization process. The identification of a serpentinized lower crust beneath the forearc of Ecuador may have crucial significance, for instance, in the definition of metallogenic zones [90].

Forward modeling seems insufficient to define the southern suture zone of the CLIP. However, by considering the different tectonic elements at the surface and subsurface, we propose that the suture zone across the Gulf of Guayaquil is most likely composed of a suture and superimposed vertical tear fault.

Throughout the use of potential field methods and the integration of different types of data, we have shown the key importance of geophysics to uncover the forearc crustal structure in Western Ecuador, such as the similar cases of southern Alaska [99], Antarctica [71, 106], Cascadia [70], and the northeast of Japan [86] where buried volcanic arcs and serpentinized mantle have also been identified based on the analyses of gravity and aeromagnetic anomalies.

Data Availability

The data used for this study are accessible at the NTNU Open Research data repository (doi:10.18710/TIJNRQ): replication data for "Forearc Crustal Structure of Ecuador Revealed by Gravity and Aeromagnetic Anomalies: Geodynamic Implications."

Disclosure

Carlos Aizprua's present address is Equinor ASA, Arkitekt Ebbells veg 10, 7053 Ranheim, Norway. This study was conducted as part of a Ph.D. thesis by C. Aizprua at the Norwegian University of Science and Technology (NTNU) in cotutelle with the University of Lille (France).

Conflicts of Interest

The authors declare no conflict of interest regarding this publication.

Acknowledgments

The funding for this work was provided by the Statoil's (currently called Equinor) AKADEMIA agreement. We are grateful to Petroamazonas EP (Quito, Ecuador) for kindly providing access to unpublished data, such as airborne gravity/magnetic and seismic data from the coastal region in Ecuador. We are thankful for Ulrike Freitag, Sofie Gradmann, and Terje Solbakk for constructive comments and corrections to the initial versions of the manuscript. Thoughtful reviews by Fabio Speranza, Fausto Ferraccioli, and editor Andrea Billi are much appreciated. Geosoft is thanked for the provision of Oasis Montaj and the GM-SYS module used for the analysis and modeling of gravity and magnetic data.

Supplementary Materials

Item DR1: anomaly enhancement and display. Item DR2: anomalies and surface exposures. Item DR3: alternative forward model. *(Supplementary Materials)*

References

[1] L. M. Boschman, D. J. J. van Hinsbergen, T. H. Torsvik, W. Spakman, and J. L. Pindell, "Kinematic reconstruction of the Caribbean region since the Early Jurassic," *Earth-Science Reviews*, vol. 138, pp. 102–136, 2014.

[2] L. Kennan and J. L. Pindell, "Dextral shear, terrane accretion and basin formation in the Northern Andes: best explained by interaction with a Pacific-derived Caribbean Plate?," *Origin and Evolution of the Caribbean Plate*, vol. 328, pp. 487–531, 2009.

[3] S. A. Whattam and R. J. Stern, "Late Cretaceous plume-induced subduction initiation along the southern margin of the Caribbean and NW South America: the first documented example with implications for the onset of plate tectonics," *Gondwana Research*, vol. 27, no. 1, pp. 38–63, 2015.

[4] C. Aizprua, C. Witt, S. E. Johansen, and D. Barba, "Cenozoic stages of forearc evolution following the accretion of a sliver from the Late Cretaceous-Caribbean large igneous province: SW Ecuador-NW Peru," *Tectonics*, vol. 38, no. 4, pp. 1441–1465, 2019.

[5] R. A. Hughes and L. F. Pilatasig, "Cretaceous and Tertiary terrane accretion in the Cordillera Occidental of the Andes of Ecuador," *Tectonophysics*, vol. 345, no. 1–4, pp. 29–48, 2002.

[6] E. Jaillard, H. Lapierre, M. Ordoñez, J. T. Álava, A. Amórtegui, and J. Vanmelle, "Accreted oceanic terranes in Ecuador; southern edge of the Caribbean Plate?," *Geological Society Special Publications*, vol. 328, no. 1, pp. 469–485, 2009.

[7] A. C. Kerr, J. A. Aspden, J. Tarney, and L. F. Pilatasig, "The nature and provenance of accreted oceanic terranes in western Ecuador: geochemical and tectonic constraints," *Journal of the Geological Society*, vol. 159, no. 5, pp. 577–594, 2002.

[8] C. Vallejo, W. Winkler, R. A. Spikings, L. Luzieux, F. Heller, and F. Bussy, "Mode and timing of terrane accretion in the forearc of the Andes in Ecuador," *Geological Society of America Memoirs*, vol. 204, pp. 197–216, 2009.

[9] C. Braz, M. Seton, N. Flament, and R. D. Müller, "Geodynamic reconstruction of an accreted Cretaceous back-arc basin in the Northern Andes," *Journal of Geodynamics*, vol. 121, pp. 115–132, 2018.

[10] L. D. A. Luzieux, F. Heller, R. Spikings, C. F. Vallejo, and W. Winkler, "Origin and Cretaceous tectonic history of the coastal Ecuadorian forearc between 1°N and 3°S: paleomagnetic, radiometric and fossil evidence," *Earth and Planetary Science Letters*, vol. 249, no. 3-4, pp. 400–414, 2006.

[11] P. Roperch, F. Megard, C. Laj, T. Mourier, T. M. Clube, and C. Noblet, "Rotated oceanic blocks in Western Ecuador," *Geophysical Research Letters*, vol. 14, no. 5, pp. 558–561, 1987.

[12] A. E. Draut and P. D. Clift, "Differential preservation in the geologic record of intraoceanic arc sedimentary and tectonic processes," *Earth-Science Reviews*, vol. 116, pp. 57–84, 2013.

[13] R. J. Stern, M. Reagan, O. Ishizuka, Y. Ohara, and S. Whattam, "To understand subduction initiation, study forearc crust: to understand forearc crust, study ophiolites," *Lithosphere*, vol. 4, no. 6, pp. 469–483, 2012.

[14] P. Clift and P. Vannucchi, "Controls on tectonic accretion versus erosion in subduction zones: Implications for the origin and recycling of the continental crust," *Reviews of Geophysics*, vol. 42, no. 2, 2004.

[15] T. Feininger and M. K. Seguin, "Simple Bouguer gravity-anomaly field and the inferred crustal structure of continental Ecuador," *Geology*, vol. 11, no. 1, pp. 40–44, 1983.

[16] J. Tamay, J. Galindo-Zaldívar, Y. M. Martos, and J. Soto, "Gravity and magnetic anomalies of Ecuadorian margin: implications in the deep structure of the subduction of Nazca Plate and Andes Cordillera," *Journal of South American Earth Sciences*, vol. 85, pp. 68–80, 2018.

[17] M. Lebrat, F. Mégard, C. Dupuy, and J. Dostal, "Geochemistry and tectonic setting of pre-collision Cretaceous and Paleogene volcanic-rocks of Ecuador," *Geological Society of America Bulletin*, vol. 99, no. 4, pp. 569–578, 1987.

[18] M. Mamberti, H. Lapierre, D. Bosch et al., "Accreted fragments of the Late Cretaceous Caribbean- Colombian Plateau in Ecuador," *Lithos*, vol. 66, no. 3-4, pp. 173–199, 2003.

[19] J. Van Melle, W. Vilema, B. Faure-Brac et al., "Pre-collision evolution of the Piñón oceanic terrane of SW Ecuador: stratigraphy and geochemistry of the "Calentura Formation"," *Bulletin De La Societe Geologique De France*, vol. 179, no. 5, pp. 433–443, 2008.

[20] L. Luzieux, "Origin and late cretaceous-tertiary evolution of the Ecuadorian forearc," Ph.D. Thesis, ETH-Zurich, 2007.

[21] E. Jaillard, M. Ordoñez, S. Benitez et al., "Basin development in an accretionary, oceanic-floored fore-arc setting: southern coastal Ecuador during late Cretaceous-late Eocene time," in *Petroleum Basins of South America*, vol. 62, American Association of Petroleum Geologists, 1995.

[22] C. Reynaud, E. Jaillard, H. Lapierre, M. Mamberti, and G. H. Mascle, "Oceanic plateau and island arcs of southwestern Ecuador: their place in the geodynamic evolution of northwestern South America," *Tectonophysics*, vol. 307, no. 3-4, pp. 235–254, 1999.

[23] H. Lapierre, D. Bosch, V. Dupuis et al., "Multiple plume events in the genesis of the peri-Caribbean Cretaceous oceanic plateau province," *Journal of Geophysical Research-Solid Earth*, vol. 105, no. B4, pp. 8403–8421, 2000.

[24] M. Lebrat, F. Megard, T. Juteau, and J. Calle, "Pre-orogenic volcanic assemblages and structure in the Western Cordillera of Ecuador between 1°40'S and 2°20'S," *Geologische Rundschau*, vol. 74, no. 2, pp. 343–351, 1985.

[25] M. Mamberti, H. Lapierre, D. Bosch, E. Jaillard, J. Hernandez, and M. Polvé, "The Early Cretaceous San Juan Plutonic Suite, Ecuador: a magma chamber in an oceanic plateau?," *Canadian Journal of Earth Sciences*, vol. 41, no. 10, pp. 1237–1258, 2004.

[26] C. Vallejo, *Evolution of the Western Cordillera in the Andes of Ecuador (Late Cretaceous-Paleogene), Eidgenoessische Technische Hochschule Zuerich*, Dissertationen, Eidgenoessische Technische Hochschule Zuerich, Zurich, Switzerland, 2007.

[27] A. Egüez, "Evolution Cenozoique de la Cordillere Occidentale septentrionale d'Equateur (0°15' S -01°10' S), les mineralisations associetees," Doc. Thesis, UPMC, Paris, 1986.

[28] P. Spadea and A. Espinosa, "Petrology and chemistry of late Cretaceous volcanic rocks from the southernmost segment of the Western Cordillera of Colombia (South America)," *Journal of South American Earth Sciences*, vol. 9, no. 1-2, pp. 79–90, 1996.

[29] C. Witt, M. Poujol, M. Chiaradia, D. Villagomez, and M. Seyler, "Evolution of the Northern Andes Cenozoic magmatic arc as recorded in the forearc detrital record," in *8th International Symposium on Andean Geodynamics (ISAG)*, Quito-Ecuador, 2019a.

[30] P. Reyes, "Relief evolution along the active margins: study of the Plio-Quaternary Deformation in the coastal Cordillera of Ecuador," Université de Nice-Sophia Antipolis – UFR Sciences, PhD Thesis, 2013.

[31] P. J. Goossens and W. I. Rose, "Chemical composition and age determination of tholeiitic rocks in the basic igneous complex, Ecuador," *Geological Society of America Bulletin*, vol. 84, no. 3, pp. 1043–1051, 1973.

[32] C. Vallejo, R. A. Spikings, B. K. Horton et al., "Chapter 8 - Late Cretaceous to Miocene stratigraphy and provenance of the coastal forearc and Western Cordillera of Ecuador: evidence for accretion of a single oceanic plateau fragment," in *Andean Tectonics*, B. K. Horton and A. Folguera, Eds., pp. 209–236, Elsevier, 2019.

[33] T. Mourier, C. Laj, F. Mégard, P. Roperch, P. Mitouard, and A. Farfan Medrano, "An accreted continental terrane in northwestern Peru," *Earth and Planetary Science Letters*, vol. 88, no. 1-2, pp. 182–192, 1988.

[34] R. J. Arculus, H. Lapierre, and É. Jaillard, "Geochemical window into subduction and accretion processes: Raspas metamorphic complex, Ecuador," *Geology*, vol. 27, no. 6, pp. 547–550, 1999.

[35] R. Spikings, R. Cochrane, D. Villagomez et al., "The geological history of northwestern South America: from Pangaea to the early collision of the Caribbean Large Igneous Province (290–75Ma)," *Gondwana Research*, vol. 27, no. 1, pp. 95–139, 2015.

[36] R. A. Spikings, P. V. Crowhurst, W. Winkler, and D. Villagomez, "Syn- and post-accretionary cooling history of the Ecuadorian Andes constrained by their in-situ and detrital thermochronometric record," *Journal of South American Earth Sciences*, vol. 30, no. 3-4, pp. 121–133, 2010.

[37] C. Witt, M. Rivadeneira, M. Poujol et al., *Tracking ancient magmatism and Cenozoic topographic growth within the Northern Andes forearc: constraints from detrital U-Pb zircon ages*, Geological Society of America Bulletin, 2017.

[38] T. Feininger, "Allochthonous terranes in the Andes of Ecuador and northwestern Peru," *Canadian Journal of Earth Sciences*, vol. 24, no. 2, pp. 266–278, 1987.

[39] L. S. Winter, R. M. Tosdal, J. K. Mortensen, and J. M. Franklin, "Volcanic stratigraphy and geochronology of the Cretaceous Lancones basin, northwestern Peru: position and timing of giant VMS deposits," *Economic Geology*, vol. 105, no. 4, pp. 713–742, 2010.

[40] J. A. Aspden, N. Fortey, M. Litherland, F. Viteri, and S. M. Harrison, "Regional S-type granites in the Ecuadorian Andes - possible remnants of the breakup of western Gondwana," *Journal of South American Earth Sciences*, vol. 6, no. 3, pp. 123–132, 1992.

[41] J. Sanchez, O. Palacios, T. Feininger, V. Carlotto, and L. Quispesivana, *Puesta en evidencia de granitoides triásicos*

en los Amotapes–Tahuín: deflexión de Huancabamba, XIII Congreso Peruano deGeologia, 2006.

[42] P. Mitouard, C. Kissel, and C. Laj, "Postoligocene rotations in southern Ecuador and northern Peru and the formation of the Huancabamba deflection in the Andean Cordillera," *Earth and Planetary Science Letters*, vol. 98, no. 3-4, pp. 329–339, 1990.

[43] P. J. Goossens, W. I. Rose, and D. Flores, "Geochemistry of tholeiites of the Basic Igneous Complex of northwestern South America," *GSA Bulletin*, vol. 88, no. 12, pp. 1711–1720, 1977.

[44] G. L. Shepherd and R. Moberly, "Coastal structure of the continental-margin, Northwest Peru and Southwest Ecuador," *Geological Society of America Memoirs*, vol. 154, pp. 351–391, 1981.

[45] M. J. Hernández, F. Michaud, J.-Y. Collot, J.-N. Proust, and E. d'Acremont, "Evolution of the Ecuador offshore nonaccretionary-type forearc basin and margin segmentation," *Tectonophysics*, vol. 781, article 228374, 2020.

[46] A. Calahorrano, V. Sallares, J. Y. Collot, F. Sage, and C. R. Ranero, "Nonlinear variations of the physical properties along the southern Ecuador subduction channel: results from depth-migrated seismic data," *Earth and Planetary Science Letters*, vol. 267, no. 3-4, pp. 453–467, 2008.

[47] J. Y. Collot, P. Charvis, M. A. Gutscher, and S. Operto, "Exploring the Ecuador-Colombia active margin and interplate seismogenic zone," *Transactions American Geophysical Union*, vol. 83, no. 17, pp. 185–190, 2002.

[48] E. R. Flueh, J. Bialas, P. Charvis, and S. S. Party, *Cruise report SO159 SALIERI*, GEOMAR, Kiel, 2001.

[49] D. Graindorge, A. Calahorrano, P. Charvis, J. Y. Collot, and N. Bethoux, "Deep structures of the Ecuador convergent margin and the Carnegie Ridge, possible consequence on great earthquakes recurrence interval," *Geophysical Research Letters*, vol. 31, no. 4, 2004.

[50] N. Bethoux, M. Segovia, V. Alvarez et al., "Seismological study of the central Ecuadorian margin: evidence of upper plate deformation," *Journal of South American Earth Sciences*, vol. 31, no. 1, pp. 139–152, 2011.

[51] Y. Font, M. Segovia, S. Vaca, and T. Theunissen, "Seismicity patterns along the Ecuadorian subduction zone: new constraints from earthquake location in a 3-D a priori velocity model," *Geophysical Journal International*, vol. 193, no. 1, pp. 263–286, 2013.

[52] M. A. Gutscher, J. Malavieille, S. Lallemand, and J. Y. Collot, "Tectonic segmentation of the North Andean margin: impact of the Carnegie Ridge collision," *Earth and Planetary Science Letters*, vol. 168, no. 3-4, pp. 255–270, 1999.

[53] A. Gailler, P. Charvis, and E. R. Flueh, "Segmentation of the Nazca and South American plates along the Ecuador subduction zone from wide angle seismic profiles," *Earth and Planetary Science Letters*, vol. 260, no. 3-4, pp. 444–464, 2007.

[54] E. Jaillard, G. Hérail, T. Monfret, and G. Wörner, "Andean geodynamics: main issues and contributions from the 4th ISAG, Göttingen," *Tectonophysics*, vol. 345, no. 1–4, pp. 1–15, 2002.

[55] C. D. Koch, C. Lynner, J. Delph et al., "Structure of the Ecuadorian forearc from the joint inversion of receiver functions and ambient noise surface waves," *Geophysical Journal International*, vol. 222, no. 3, pp. 1671–1685, 2020.

[56] C. Lynner, C. Koch, S. L. Beck et al., "Upper-plate structure in Ecuador coincident with the subduction of the Carnegie Ridge and the southern extent of large mega-thrust earthquakes," *Geophysical Journal International*, vol. 220, no. 3, pp. 1965–1977, 2019.

[57] F. Michaud, J.-Y. Royer, and C. Witt, "Influence of the subduction of the Carnegie volcanic ridge on Ecuadorian geology: reality and fiction," in *Backbone of the Americas: Shallow Subduction, Plateau Uplift, and Ridge and Terrane Collision*, V. A. R. Suzanne Mahlburg Kay and R. D. William, Eds., pp. 217–228, Geological Society of America, 2009.

[58] C. Witt and J. Bourgois, "Forearc basin formation in the tectonic wake of a collision-driven, coastwise migrating crustal block: the example of the North Andean block and the extensional Gulf of Guayaquil-Tumbes Basin (Ecuador-Peru border area)," *Geological Society of America Bulletin*, vol. 122, no. 1-2, pp. 89–108, 2010.

[59] E. Sanclemente, "Seismic imaging of the structure of the Central Ecuador convergent margin : relationship with the interseismic coupling variations," Docteur en sciences: Université Nice Sophia Antipolis, 2014.

[60] W. J. Hinze, R. R. B. von Frese, and A. H. Saad, *Gravity and Magnetic Exploration: Principles, Practices, and Applications*, Cambridge University Press, Cambridge, 2013.

[61] L. C. G. Cano, A. Galve, P. Charvis, and B. Marcaillou, "Three-dimensional velocity structure of the outer fore arc of the Colombia-Ecuador subduction zone and implications for the 1958 megathrust earthquake rupture zone," *Journal of Geophysical Research: Solid Earth*, vol. 119, no. 2, pp. 1041–1060, 2014.

[62] J. Y. Collot, W. Agudelo, A. Ribodetti, and B. Marcaillou, "Origin of a crustal splay fault and its relation to the seismogenic zone and underplating at the erosional north Ecuador-south Colombia oceanic margin," *Journal of Geophysical Research-Solid Earth*, vol. 113, no. B12, 2008.

[63] A. C. Mix, R. Tiedemann, P. Blum et al., *Leg 202 summary: Proceedings of the Ocean Drilling Program, initial reports, Southeast Pacific paleoceanographic transects; covering Leg 202 of the cruises of the drilling vessel JOIDES Resolution*, vol. 202, Valparaiso, Chile, to Balboa, Panama; sites 1232-1242, 29 March-30 May 2002, 2003.

[64] C. D. R. Evans and J. E. Whittaker, "The geology of the western part of the Borbón Basin, North-west Ecuador," *Special Publications*, vol. 10, no. 1, pp. 191–198, 1982.

[65] C. Witt, J. Bourgois, F. Michaud, M. Ordonez, N. Jimenez, and M. Sosson, "Development of the Gulf of Guayaquil (Ecuador) during the Quaternary as an effect of the North Andean block tectonic escape," *Tectonics*, vol. 25, no. 3, 2006.

[66] N. Espurt, S. Brusset, P. Baby et al., "Deciphering the Late Cretaceous-Cenozoic structural evolution of the North Peruvian forearc system," *Tectonics*, vol. 37, no. 1, pp. 251–282, 2018.

[67] A. Alvarado, L. Audin, J. M. Nocquet et al., "Partitioning of oblique convergence in the Northern Andes subduction zone: migration history and the present-day boundary of the North Andean Sliver in Ecuador," *Tectonics*, vol. 35, no. 5, pp. 1048–1065, 2016.

[68] D. Bosch, P. Gabriele, H. Lapierre, J.-L. Malfere, and E. Jaillard, "Geodynamic significance of the Raspas Metamorphic Complex (SW Ecuador): geochemical and isotopic constraints," *Tectonophysics*, vol. 345, no. 1–4, pp. 83–102, 2002.

[69] L. P. Beard, "Detection and identification of north–south trending magnetic structures near the magnetic equator," *Geophysical Prospecting*, vol. 48, no. 4, pp. 745–761, 2000.

[70] R. J. Blakely, T. M. Brocher, and R. E. Wells, "Subduction-zone magnetic anomalies and implications for hydrated forearc mantle," *Geology*, vol. 33, no. 6, pp. 445–448, 2005.

[71] F. Ferraccioli, E. Bozzo, and G. Capponi, "Aeromagnetic and gravity anomaly constraints for an early Paleozoic subduction system of Victoria Land, Antarctica," *Geophysical Research Letters*, vol. 29, no. 10, pp. 44-1–44-4, 2002.

[72] S. Benitez, *Évolution géodynamique de la province côtière sud-équatorienne au Crétacé supérieur-Tertiaire*, Université Joseph-Fourier - Grenoble I, 1995.

[73] J.-Y. Collot, M. J. Hernandez Salazar, F. Michaud, J.-N. Proust, R. Ortega, and A. M. Aleman, *The Neogene forearc basins of the Ecuadorian Shelf (1 degrees N-2 degrees 20'S); preliminary interpretation of a dense grid of MCS data*, American Geophysical Union Fall Meeting, 2014.

[74] M. Ordónez, N. Jiménez, and J. Suárez, *Micropaleontología ecuatoriana. datos bioestratigráficos y paleoecológicos de las cuencas: Graben de Jambelí, Progreso, Manabí, Esmeraldas y Oriente; del levantamiento de la península de Santa Elena, y de las cordilleras Chongón Colonche, costera y Occidental, Quito, Ecuador*, Petroproducción y Centro de Investigaciones Geológicas de Guayaquil, 2006.

[75] N. Lucas and D. Delgado, *Análisis tectono-estratigráfico de la Cuenca Borbón-Esmeraldas: Noroeste de Ecuador Ingeniero*, Escuela Superior Politécnica del Litoral, 2018.

[76] B. Marcaillou and J. Y. Collot, "Chronostratigraphy and tectonic deformation of the North Ecuadorian-South Colombian offshore Manglares forearc basin," *Marine Geology*, vol. 255, no. 1-2, pp. 30–44, 2008.

[77] Y. Deniaud, "Enregistrements sédimentaire et structural de l'évolution géodynamique des Andes équatoriennes au cours du Néogène : étude des bassins d'avant-arc et bilans de masse," PhD Thesis: Université Joseph Fourier, 2000.

[78] J. L. Tetreault and S. J. H. Buiter, "Future accreted terranes: a compilation of island arcs, oceanic plateaus, submarine ridges, seamounts, and continental fragments," *Solid Earth*, vol. 5, no. 2, pp. 1243–1275, 2014.

[79] C. Witt, J. Y. Reynaud, D. Barba et al., "From accretion to forearc basin initiation: the case of SW Ecuador, Northern Andes," *Sedimentary Geology*, vol. 379, pp. 138–157, 2019.

[80] R. D. Hyndman and S. M. Peacock, "Serpentinization of the forearc mantle," *Earth and Planetary Science Letters*, vol. 212, no. 3-4, pp. 417–432, 2003.

[81] P. B. Toft, J. Arkani-Hamed, and S. E. Haggerty, "The effects of serpentinization on density and magnetic susceptibility: a petrophysical model," *Physics of the Earth and Planetary Interiors*, vol. 65, no. 1-2, pp. 137–157, 1990.

[82] A. H. Saad, "Magnetic properties of ultramafic rocks from Red Mountain, California," *Geophysics*, vol. 34, no. 6, pp. 974–987, 1969.

[83] B. Reynard, "Serpentine in active subduction zones," *Lithos*, vol. 178, pp. 171–185, 2013.

[84] T. Seno, "Variation of downdip limit of the seismogenic zone near the Japanese islands: implications for the serpentinization mechanism of the forearc mantle wedge," *Earth and Planetary Science Letters*, vol. 231, no. 3-4, pp. 249–262, 2005.

[85] C. Vallejo, F. Soria, F. Tornos et al., "Geology of El Domo deposit in central Ecuador: a VMS formed on top of an accreted margin," *Mineralium Deposita*, vol. 51, no. 3, pp. 389–409, 2016.

[86] C. Finn, "Aeromagnetic evidence for a buried Early Cretaceous magmatic arc, northeast Japan," *Journal of Geophysical Research: Solid Earth*, vol. 99, no. B11, pp. 22165–22185, 1994.

[87] M. Chiaradia, "Adakite-like magmas from fractional crystallization and melting-assimilation of mafic lower crust (Eocene Macuchi arc, Western Cordillera, Ecuador)," *Chemical Geology*, vol. 265, no. 3-4, pp. 468–487, 2009.

[88] R. A. Hughes, R. Bermúdez, and G. Espinel, *Mapa Geológico de la Cordillera Occidental del Ecuador entre 0°-1°S*, BGS & CODIGEM, scale 1:200.000, 1999.

[89] W. J. McCourt, P. Duque, L. F. Pilatasig, and R. Villagómez, *Mapa Geológico de la Cordillera Occidental del Ecuador entre 1°-2°S*, BGS & CODIGEM, scale 1:200.000, 1999.

[90] J. P. Richards, "Postsubduction porphyry Cu-Au and epithermal Au deposits: products of remelting of subduction-modified lithosphere," *Geology*, vol. 37, no. 3, pp. 247–250, 2009.

[91] J. P. Richards, "Magmatic to hydrothermal metal fluxes in convergent and collided margins," *Ore Geology Reviews*, vol. 40, no. 1, pp. 1–26, 2011.

[92] D. Bonnemains, J. Carlut, J. Escartín, C. Mével, M. Andreani, and B. Debret, "Magnetic signatures of serpentinization at ophiolite complexes," *Geochemistry, Geophysics, Geosystems*, vol. 17, no. 8, pp. 2969–2986, 2016.

[93] M. G. Petterson, "A review of the geology and tectonics of the Kohistan island arc, North Pakistan," *Geological Society, London, Special Publications*, vol. 338, no. 1, pp. 287–327, 2010.

[94] E. Lopez, *Evolution tectono-stratigraphique du double bassin avant-arc de la marge convergente Sud Colombienne - Nord Equatorienne pendant le Cénozoïque Diplôme*, Université de Nice Sophia Antipolis, 2009.

[95] F. Cediel, R. P. Shaw, C. Cáceres, C. Bartolini, R. T. Buffler, and J. F. Blickwede, *Tectonic assembly of the northern Andean block, The Circum-Gulf of Mexico and the Caribbean: Hydrocarbon Habitats, Basin Formation and Plate Tectonics, Volume 79*, American Association of Petroleum Geologists, 2003.

[96] W. D. MacDonald, J. J. Estrada, and G. Humberto, "Paleoplate affiliations of volcanic accretionary terranes of the northern Andes: abstracts with programs," *Geological Society of America*, vol. 29, no. 6, p. 45, 1997.

[97] A. C. Kerr, "La Isla de Gorgona, Colombia: a petrological enigma?," *Lithos*, vol. 84, no. 1–2, pp. 77–101, 2005.

[98] A. C. Kerr and J. Tarney, "Tectonic evolution of the Caribbean and northwestern South America: the case for accretion of two Late Cretaceous oceanic plateaus," *Geology*, vol. 33, no. 4, pp. 269–272, 2005.

[99] N. Mankhemthong, D. I. Doser, and T. L. Pavlis, "Interpretation of gravity and magnetic data and development of two-dimensional cross-sectional models for the Border Ranges fault system, south-central Alaska," *Geosphere*, vol. 9, no. 2, pp. 242–259, 2013.

[100] J. Bourgois, "A review on tectonic record of strain buildup and stress release across the Andean forearc along the Gulf of Guayaquil-Tumbes Basin (GGTB) near Ecuador-Peru border," *International Journal of Geosciences*, vol. 4, no. 3, pp. 618–635, 2013.

[101] P. Herms, T. John, R. J. Bakker, and V. Schenk, "Evidence for channelized external fluid flow and element transfer in subducting slabs (Raspas Complex, Ecuador)," *Chemical Geology*, vol. 310–311, pp. 79–96, 2012.

[102] T. John, E. E. Scherer, V. Schenk, P. Herms, R. Halama, and D. Garbe-Schönberg, "Subducted seamounts in an eclogite-facies ophiolite sequence: the Andean Raspas Complex, SW Ecuador," *Contributions to Mineralogy and Petrology*, vol. 159, no. 2, pp. 265–284, 2010.

[103] D. Boutelier and A. Chemenda, *Physical modeling of arc–continent collision: a review of 2D, 3D, purely mechanical and thermo-mechanical experimental models, Arc-Continent Collision*, Springer Berlin Heidelberg, Berlin, Heidelberg, 2011.

[104] J. F. Dumont, E. Santana, and W. Vilema, "Morphologic evidence of active motion of the Zambapala Fault, Gulf of Guayaquil (Ecuador)," *Geomorphology*, vol. 65, no. 3–4, pp. 223–239, 2005.

[105] M. J. Hernández Salazar, J. N. Proust, E. D'Acremont, F. Michaud, and J. Y. Collot, "Neogene evolution of western boundary of the Manabí basin controlled by the Jama Fault System," in *8th International Symposium on Andean Geodynamics (ISAG)*, Quito-Ecuador, 2019.

[106] F. Ferraccioli, P. C. Jones, A. P. M. Vaughan, and P. T. Leat, "New aerogeophysical view of the Antarctic Peninsula: more pieces, less puzzle," *Geophysical Research Letters*, vol. 33, no. 5, 2006.

[107] T. Aitken, P. Mann, A. Escalona, and G. L. Christeson, "Evolution of the Grenada and Tobago basins and implications for arc migration," *Marine and Petroleum Geology*, vol. 28, no. 1, pp. 235–258, 2011.

[108] D. T. Sandwell, R. D. Muller, W. H. F. Smith, E. Garcia, and R. Francis, "New global marine gravity model from CryoSat-2 and Jason-1 reveals buried tectonic structure," *Science*, vol. 346, no. 6205, pp. 65–67, 2014.